Functional characterization of novel regulators required for genomic integrity

Bachelor thesis

submitted to the
Faculty of Bio Sciences
of the Ruperto-Carola University of Heidelberg, Germany
for the degree
Bachelor of Science (B.Sc.)

Christoph Budjan
2008

Christoph Budjan[1,2]

[1]German Cancer Research Center (DKFZ), Division of Signaling and Functional Genomics and Heidelberg University, Department of Cell and Molecular Biology, Medical Faculty Mannheim, Heidelberg, Germany
[2]Current address: Gurdon Institute, University of Cambridge, CB2 1QN, Cambridge, United Kingdom
Email: cb631@cam.ac.uk

This thesis was submitted to the Undergraduate program in Biology at the University of Heidelberg, Germany in June, 2008 for the degree Bachelor of Science.
Experimental design and ideas were developed together with Michael Boutros and Florian Fuchs. Florian Fuchs acted as a primary supervisor in the lab.
The thesis project followed from a primary screen that Florian Fuchs developed and which was performed together with myself and others in the Boutros lab. A significant part of the results from my project were later published as part of a paper entitled “Clustering phenotype populations by genome-wide RNAi and multiparametric imaging.” published in *Mol Syst Biol* **6**, 370 (doi: 10.1038/msb.2010.25).

Table of contents

Summary

Post-genomic approaches such as RNAi are nowadays widely utilized methods to systematically analyze loss-of-function phenotypes and functionally annotate novel genes. Apart from homogeneous readouts such as pathway-specific reporter assays, high-content microscopy is increasingly recognized as a powerful tool to analyze cell-based perturbation phenotypes in a high-throughput manner.

We have conducted a genome-wide RNAi screen using automated microscopy and image analysis to classify single cells into phenotypic classes based on their multidimensional morphological signatures. Using an optimized metric of phenotype similarity, we could associate previously uncharacterized genes with known functional modules. To validate our findings from the primary screen and further functionally characterize genes from a phenotypic cluster exhibiting strong viability effects and cell-cycle arrest, I performed high-throughput *in situ* cytometry after knockdown of gene products and looked for synthetic effects after DNA-damage inducing IR irradiation. To compare and identify putative conserved functions of our candidate genes, I also analyzed fly cells after depletion of homologous genes for cell cycle and viability phenotypes similar to their human homolog.

Because of strong cell cycle effects observed in some siRNA-depleted genes, I next performed immunofluorescence microscopy to look for activation of DNA damage response following depletion of protein levels in combination with DNA damage inducing agents. Interestingly, nuclei foci formation could be observed in some of the cells after only RNAi treatment, suggesting a role in regulating and monitoring genomic integrity.

Finally, I performed localization studies of *Donson*, a candidate gene which was found in one of our clusters with strong viability and cell cycle effects from the primary screen. HA-tagged *Donson* was visible at the perinuclear region in two distinct foci, reminiscent of centrioles localization, suggesting a previously unanticipated mechanism of regulation and localization of *Donson*.

Quantitative automated analysis of perturbation phenotypes on a genome-wide scale provides means to annotate unknown genes by categorizing them into known modules based on their phenotypic profile and will significantly influence and accelerate functional genetic studies as well as drug discovery in the years to come.

1 Introduction

1.1 Analysis of cell morphology by RNAi

Cell shape is determined by a multitude of factors all contributing to the final outcome of a cellular phenotype. Depending on the cell cycle phase and type and, most notably on regulatory proteins of the actin cytoskeleton and microtubules, cellular phenotypes even within one cell population can vary dramatically. To understand basic morphogenetic events on a cellular level, cultured cells have been widely used to characterize genes important for regulation of the cytoskeleton, protein secretion, cell-cycle and cell motility (Scales 1997; Hartwell, 1973; reviewed in Raftopoulou and Hall, 2003).

With the availability of whole genome sequences, targeted perturbation technologies have facilitated the functional annotation of uncharacterized genes, which in the time of the post-genomic era, is one of the current frontiers in biological sciences. Arguably the most promising reverse genetic approach which has emerged in recent years is RNA interference (RNAi). RNAi is a post-transcriptional gene silencing mechanism present in most eukaryotes from worms and flies to man (Hannon, 2002). It was first described as a defense mechanism in which double-stranded (ds) RNA targets homologous mRNAs for degradation via an endogenous degradation machinery (Fire, 1998). With the availability of genome-covering RNAi libraries in various organisms it is now possible to systematically analyze loss-of-function phenotypes on a genome-wide scale (Boutros, 2004; Berns, 2004).

Since the first discovery of RNAi in plants (van der Krol, 1990; Napoli, 1990), much effort has been put into the elucidation of its underlying mechanisms. Several studies showed that introducing long dsRNA into cells leads to their cleavage into short interfering RNAs (siRNAs) of approximately 22 nucleotides length, a process which is mediated by the *RNAseIII* endonuclease Dicer (Ketting et al., 2001; Bernstein et al., 2001). Following the cleavage of dsRNA into siRNAs, siRNAs get incorporated into the RNA-induced silencing complex (RISC), which unwinds the RNA duplex via its helicase-activity. The single-stranded siRNA (also known as 'guide' strand) binds to its target mRNA in a RISC-dependent manner which gets cleaved by the RISC *RNaseH* nuclease activity (see figure 1; Hammond et al, 2000).

First RNAi experiments were successfully performed in the nematode *Caenorhabditis elegans* (Fire et al., 1998) and uptake methods of dsRNAs were subsequently improved. Initial experiments were done by injecting long dsRNAs (approximately 500 bp) into worms, later by feeding bacteria expressing dsRNAs or by soaking them directly in solution containing dsRNA (reviewed in Hannon, 2002; Timmons and Fire, 1998). In *Drosophila melanogaster*, similar methods were used, either by injecting dsRNA into embryos or by stably introducing dsRNA hairpins in transgenic flies (Kennerdell and Carthew, 1998; 2000; Tavernarakis et al., 2000).

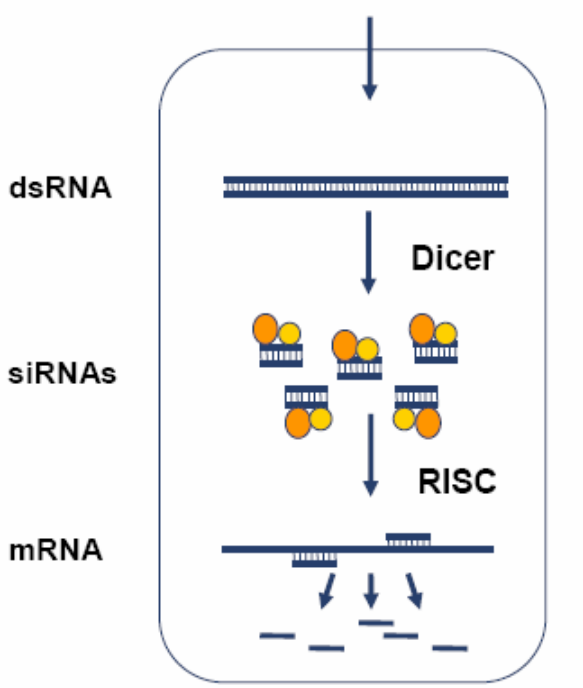

Figure 1 RNAi mechanism. see text for details.

Adapting the RNAi technology to the mammalian system was initially prevented by the fact that introducing long dsRNA into mammalian cells triggers innate immune pathways including interferon-regulated responses that serve as an antiviral mechanism. Additionally, the dsRNA-dependent protein kinase (PKR) binds dsRNA and catalyzes sequence-independent RNA degradation and general proteins synthesis inhibition (Williams, 1997). Increasing biochemical understanding of the RNAi machinery lead to the realization that dsRNA shorter than 30 bp could induce the sequence-specific RNAi pathway without the undesired effects of innate immune responses (Elbashir et al., 2001). Apart from chemically synthesized siRNAs of 21 nt length, generation of stemloop-containing short hairpin RNAs (shRNAs) which

mimic the endogenous counterpart of siRNAs - microRNAs (miRNAs) - were successfully designed and could be used to stably express siRNA in cultured cells and tissues (Paddison, 2002). Bishop and colleagues developed another method of siRNA production by in vitro-"dicing" long dsRNAs using *E.coli RNase III* enzyme to generate endoribonuclease-prepared siRNAs (esiRNAs) (Yang et al., 2002).

Certain pitfalls in using the RNAi technology to analyze loss-of-function phenotypes still remain today, probably the most important being so-called off-target effects (OTEs). Sequence-independent and dependent OTEs were early recognized phenomena, but the magnitude of these effects was only realized in recent years. Reports which showed silencing of non-targeted genes with only short perfect matches, or matches of 3' untranslated region (UTR) of transcripts with seed regions of siRNAs (position 2-7 and 2-8, respectively) and siRNAs functioning as miRNAs through non-perfect matches questioned previously published 'hitlists' of genome-wide RNAi screens (Birmingham et al., 2006; Jackson et al., 2003; Doench et al., 2003). Several guidelines based on a general consensus have been developed in order to minimize misinterpretation of RNAi experiments and to verify data obtained from loss-of-function phenotypic readouts (Cullen, 2006; Echeverri and Perrimon, 2006). Examples are the use of sequence-independent siRNAs targeting the same transcript and rescue experiments in which the RNAi-induced phenotype is countered by expression of a functional version of the gene that is resistant to the siRNA (Echeverri et al., 2006).

Through the availability of large-scale RNAi libraries covering almost the entire genome of various species including *Drosophila*, *C. elegans* and man, it is possible to screen for novel genes acting in a particular pathway or process using cell-based reporter assays based on specific activation of a luciferase gene upon pathway stimulation (Mueller et al., 2005; Bartscherer et al., 2006). Other phenotypic readouts include detection of changes in cell viability by directly measuring the ATP level of a given cell population (Boutros et al., 2004) and morphology screens based on automated image acquisition (Kiger et al., 2003; Bakal et al., 2007).

1.2 Image-based screening

In recent years, high-content screening based on automated microscopy has emerged as an important phenotypic readout method for large-scale perturbation experiments using RNAi or chemical compounds. This relatively young branch of high-throughput screens owes its increasing use and popularity not only technological advances but also improvements in computational analysis algorithms which are important for any post-acquisition step required to interpret large image datasets (reviewed in Wollman and Stuurman, 2007). Compared to focused reporter assays used to identify novel genes implicated in a particular pathway of interest, high-content screenings are more sensitive and generally applicable and are less prone to false-positive 'hits' which is a general issue in large-scale RNAi screens. Provided that suitable antibodies are available, subtle phenotypic changes in cell morphology and subcellular localization of proteins can be monitored in a spatiotemporal manner which would otherwise be unnoticed in focused reporter assays (Huang and Murphy, 2004; Neumann et al., 2006). Besides higher costs because of expensive probes used and relatively limited throughput due to longer image-acquisition times, microscopy-based screens generate large amounts of data which require sufficient data storage capabilities and suitable image analysis software which often needs to be adapted to the phenotypic readout, cell line and screening protocol.

Image analysis software extracts and measures specific characteristics in multiple cells to convert obtained images into statistically relevant data. For this, a binary image is generated based on different threshold and edge-detection methods to distinguish objects of interest from background. Subsequently, individual cells are labeled, such that each cell has its own identifier. Finally regions of interest - usually cell nucleus and cytoplasm - are segmented, often using nuclei as seed regions to avoid over-segmentation (Wollman et al., 2007; Goshima et al., 2007). Following the segmentation step, cells can be classified into subsets of phenotypic classes. Computer-based labeling of cells requires generation of a classifier trainingsset in which individual classes are defined based on their unique descriptor profile by manually labeling a small sample of cells (Figure 2). This kind of procedure is called supervised learning and is distinct from unsupervised learning in which the computer divides a given number of cells into subsets without prior training. To classify cells, the computer extracts a set of descriptors or image features such as nuclear size,

fluorescence intensity in different subcellular regions, mixed features based on multiple channels which describe morphological characteristics like eccentricity and texture features.

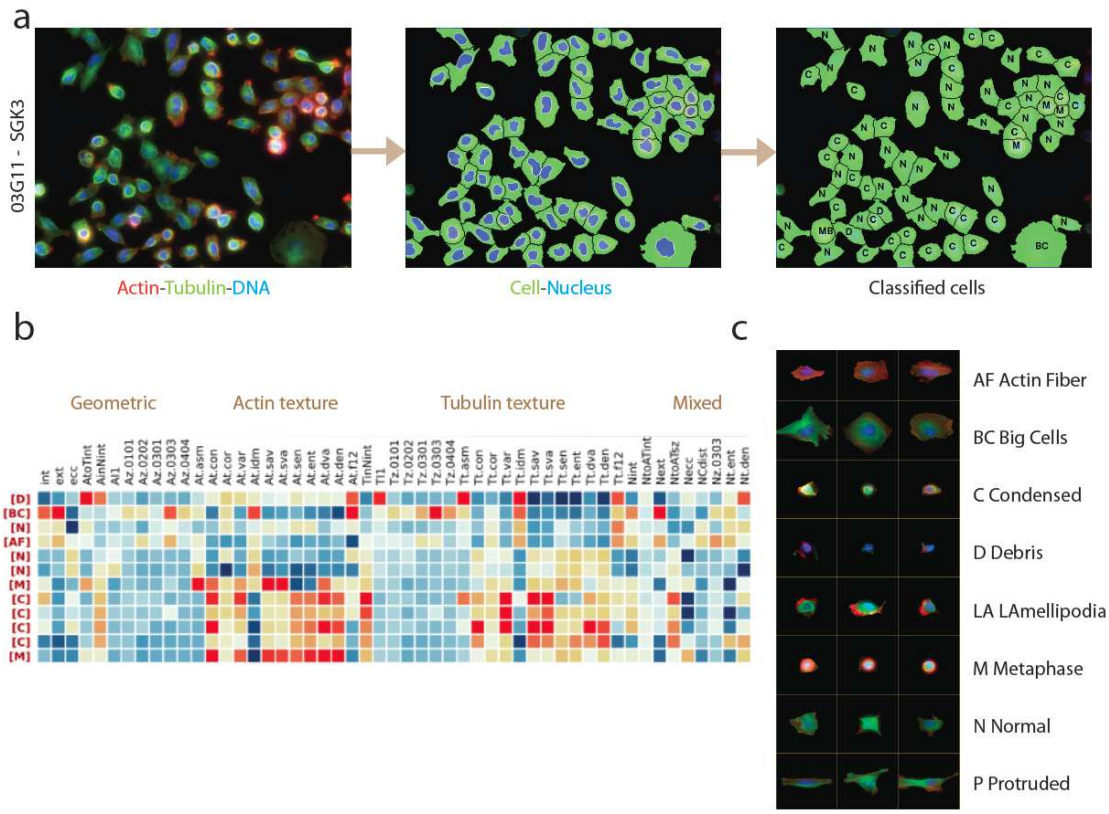

Figure 2 From raw images to classification. (a) Image analysis workflow showing sample images of segmented and classified cells. (b) Phenotypic profiles of single cells assign them to predefined classes. (c) Example images from the classifier trainingsset used to describe different phenotypic classes

There are two approaches one can use to score phenotypes. If you have a specific hypothesis then one only has to measure characteristics relevant for their hypothesis. For instance, one RNAi screen in *Drosophila* cells performed by Goshima and colleagues used γ-tubulin-stained centrosomes to look for changes in spindle length to identify novel genes involved in spindle assembly (Goshima et al., 2007). Another approach is to look for any morphological changes without having a prior hypothesis (Tanaka et al., 2005; Bakal et al., 2007). Using this unbiased approach one can potentially identify genes involved in diverse cellular processes such as cell motility and polarity, cell cycle regulation and apoptosis.

High-content approaches are becoming increasingly attractive in drug discovery as a quantitative tool for target prediction (Eggert et al., 2004), mechanism of action (Young et al., 2007) and assessment of drug effects on a single-cell level (Perlman et al., 2004). Combining small molecule and genome-wide RNAi screens, target predictions can be made based on phenotypic similarities to multivariate loss-of-function phenoprints of RNAi-mediated perturbation screens. Cytotoxic versus pharmacological activity of small molecules at a certain concentration, a key parameter in drug development, can be efficiently established at a level of the cellular phenotype using different dilutions for dose-response profiling chemical compounds (Starkuviene and Pepperkok, 2007; Perlman et al., 2004).

1.3 DNA damage response and genome surveillance mechanisms

The genome is under constant thread by exogenous damage inducing agents and errors during replication. Therefore, it might not be surprising that all higher organisms have conserved DNA damage repair pathways and surveillance mechanisms which assure genomic integrity throughout cell cycle progression (Sancar et al., 2005). Deregulation of and mutations in genes required for the DNA damage response (DDR) pathway are often associated with the development of cancer (Vermeulen et al., 2003).

Depending on the type of DNA damage, various repair mechanisms ensure correction of double-strand breaks, mismatches during DNA replication, DNA adducts and base damage. Central to the regulation of these DDR pathways during different cell cycle phases are so called cell-cycle checkpoints. Checkpoints primarily promote cell-cycle delay, thereby providing time for the repair process and preventing integration of DNA lesions and mismatches in the following cell generations. Increasing evidence points to a more mutual role of checkpoint proteins in the propagation of the DNA damage signal and activation of DDR (Bartek et al., 2004). Diverse and partly overlapping checkpoint pathways control crucial transition steps between G1 and S, and G2/M, respectively, as well as during replication.

The initial step of checkpoint and DDR activation is mediated by DNA-damage sensing complexes which recognize different types of DNA damage and propagate the signal to downstream checkpoint kinases and repair enzymes by

recruiting them to DNA damage sites. Double-strand breaks (DSBs) are sensed by the MRE11-RAD50-NBS1 (MRN) complex which recruits the protein kinase ataxia telangiectasia mutated (ATM) to sites of DNA damage (D'Amours and Jackson, 2002). ATM undergoes autophosphorylation and activated ATM phosphorylates H2AX, a H2A histone variant. At DSBs, γH2AX (the phosphorylated form of H2AX) recruits additional ATM molecules in a positive feedback loop. Important for the establishment of this positive feedback loop are MDC1 and 53BP1, so-called mediators of DDR signaling which promote recruitment of ATM complexes to γH2AX (Lukas et al., 2004; Stucki et al., 2005; Abraham, 2002).

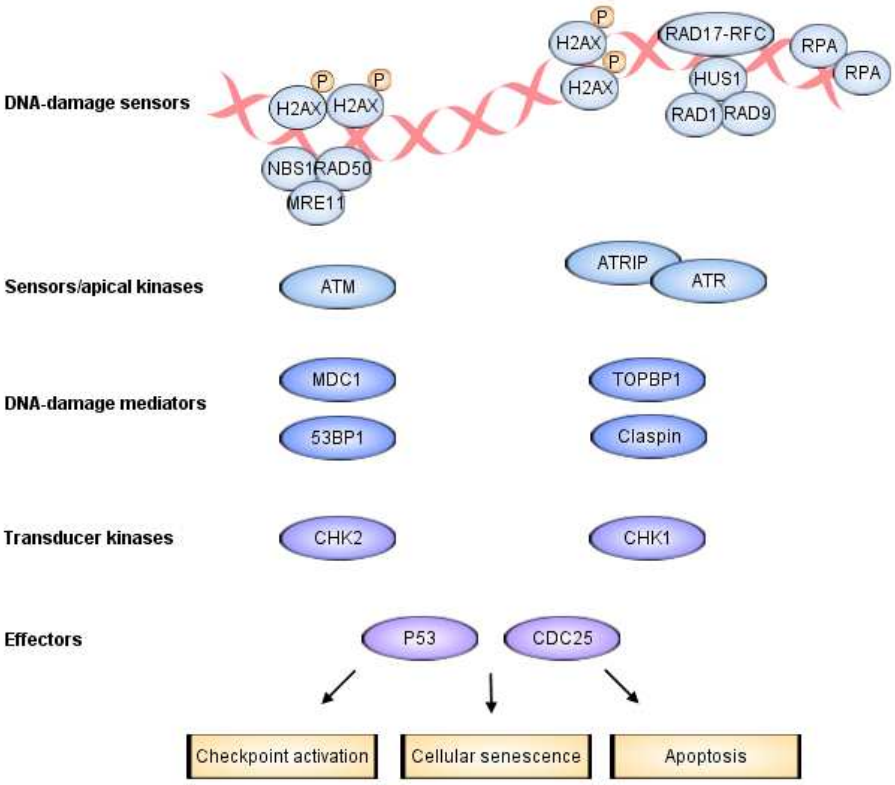

Figure 3 The DNA-damage response. DDR signaling is activated upon DNA double-strand breaks (DSBs) or RPA-coated single-stranded DNA which induce different downstream branches of the DNA-damage response ultimately leading to transient cell cycle arrest or cellular senescence and apoptosis if the DNA insult is too severe or DNA-damage signaling persists for a longer time period. See text for details. 53BP1, p53-binding protein 1; ATM, ataxia telangiectasia mutated; ATR, ataxia telangiectasia and Rad3-related; ATRIP, ATR-interacting protein; DDR, DNA damage response; DSB, double-strand break; MDC1, mediator of DNA-damage checkpoint 1; MRE11, meiotic recombination 11; NBS1, Nijmegen breakage syndrome 1; RPA, replication protein A; RFC, replication factor C; TOPBP1, DNA topoisomerase-II-binding protein 1. Figure adapted from Campisi et al., 2007.

Collapse of stalled replication forks or gaps generated during S-phase lead to single-stranded DNA which is immediately coated by polymers of Replication protein A (RPA). RPA-coated single-stranded DNA then promotes the recruitment of heterodimeric complexes consisting ATM and Rad3-related (ATR) and its DNA-binding protein, ATR-interacting protein (ATRIP). Although no similar feedback loop for ATR has been proposed, ATR activity is amplified by additional ATR targets, such as RAD9-HUS1-RAD1 (9-1-1) and RAD17-RFC complexes (Weiss et al., 2002). Additionally, ATR activity is stimulated by TOPB1, a DNA damage mediator protein, and Claspin, which is required for CHK1 phosphorylation by ATR (Kumagai et al., 2006; Liu et al., 2006).

In contrast to upstream DDR signaling factors, CHK2 and CHK1, the downstream transducer kinases of ATM and ATR-dependent DNA-damage signaling, are only transiently localizing to sites of DNA damage and diffuse freely into more distant parts inside the nucleus after their activation to propagate the DNA damage signal by phosphorylation and activation of effector proteins, such as p53 and CDC25 phosphatases, thereby connecting DDR with cell cycle regulation and progression.
CDC25 phosphatases are required for normal cell cycle progression through activation of CDKs and their inactivation causes a rapid cell-cycle arrest. DDR-mediated inactivation of CDC25 is regulated by either proteolytic degradation or exclusion from the nucleus. p53 induces and is maintaining cell-cycle arrest by activating the transcription of p21, a Cyclin-dependent kinase (CDK)-inhibitor that prevents G1/S transition.

After successful completion of DNA-repair, DDR complexes are disassembled to allow re-initiation of replication and cell proliferation. This is mediated by both, chromatin remodeling and de-phosphorylation of γH2AX complexes (Downey et al., 2006). Cells with irreparable DNA damage or sustained cell-cycle arrest can also induce apoptosis or go into a state called cellular senescence, in which cells are still metabolic active but have lost their ability to proliferate (Campisi et al., 2007).

1.4 Aim of this thesis and experimental approach

Morphogenetic events play important roles during tissue remodeling, development and diseases such as cancer. Understanding molecular mechanisms underlying diverse cellular cell shape changes will give better insights into disease-related morphogenesis and will help in identifying suitable drug targets for therapeutic intervention. So far, classical forward genetic screens have identified numerous genes important for as diverse processes as cell-cycle, secretion, signal-transduction, DNA-damage response and many others. With the advent of RNAi it is now possible to systematically and rapidly investigate gene function based on available sequences of popular model organisms as well as man and categorize novel genes to known functional modules (Hartwell et al., 1999; Spirin and Mirny, 2003).

We recently performed a genome-wide RNAi screen in human cells using automated microscopy and image-based analysis to identify novel genes involved in cell shape regulation, cell-cycle progression and cell survival (Fuchs et al., 2008). Clustering of multi-dimensional phenotypic profiles based on an optimized distance metric enables us to infer protein function by similarity of perturbation phenotypes on a single-cell level. For functional analysis of a phenotypic cluster around a previously uncharacterized gene, named downstream neighbor of Son (Donson), which showed strong viability effects and cell-cycle arrest phenotype, I conducted secondary assays assessing observed cell-cycle effects as well as investigate a putative role of those genes in DNA repair and genomic surveillance mechanisms.

The aim of my thesis thus was, to further characterize potential candidate genes in secondary assays using the RNAi technology in combination with DNA damage inducing drugs to confirm and investigate our hypothesized gene functions based on known genes from our cluster of interest. My strategy was to

1. Perform high-throughput in-situ cytometry to confirm cell-cycle phenotypes we observed in our microscopy screen and further characterize putative roles of genes in particular cell-cycle phases e.g. by regulating checkpoint signaling, replication or mitosis.

2. Compare obtained cell-cycle data from human cells with *Drosophila* homologs using flow-cytometry to see if there might be functional conservation of those genes.

3. Analyze putative roles of our candidate genes in DNA repair and genomic surveillance mechanisms using fluorescence microscopy to check for an activation of DNA damage response.

4. Develop cloning strategies for Donson, an uncharacterized gene with a very strong viability phenotype, to perform rescue studies with the mouse homolog and localization studies using a tagged version of this gene.

Morphological events leading to changes in cell polarity, cytoskeletal rearrangements and cell shape are poorly understood at a molecular level. Identification of novel genes required for genomic integrity, cell survival and polarity changes during various states of the cell including events leading to mitosis will accelerate functional genomic research and might also influence cancer research. Newly identified genes might constitute bona-fide drug targets and thus the initial step towards drug discovery and development.

2 Results

2.1 Genome-wide RNAi survey for changes in cell morphology

RNAi technology and the availability of genome-wide RNAi libraries in combination with suitable reporter assays has made it possible to systematically and rapidly screen for novel genes acting in known pathways. To identify genes implicated in known processes based on cell morphology changes upon gene perturbations, we conducted a large-scale RNAi survey in human cells targeting almost all transcripts of the human genome. Following 48 hours of RNAi treatment, cells were fixed and stained for DNA, actin and tubulin. Image data was obtained using automated microscopy. Overall, 600,000 images were obtained and analyzed. Subsequently, individual cells were segmented and assigned into one of eight predefined phenotypic classes based on multi-dimensional parameters which allowed us to distinguish subtle differences between classes with high similarity, e.g. condensed and mitotic cells (see Figure 1a-c). Phenotypic classes, including cells in meta- or telophase, large and condensed cells, cells with elongation/protrusions or lamellipodia, and cell debris, were defined using a supervised training algorithm and a manually selected set of individual cells for each class to train a classifier. RNAi knockdown of 21,125 genes gave rise to a variety of different phenoprints which could be compared in terms of their phenotypic distance to each other. From this, we could generate a multi-dimensional phenotypic landscape describing phenotypic effects of gene perturbations on cell morphology for almost all genes in the human genome.

For secondary assays and functional annotation of unknown genes, we had a closer look at tight clusters with striking phenotypes such as a high penetration of single phenotypic classes and genes which exhibited cell cycle effects. Among our candidate gene list were two phenotypic gene centered clusters. The first cluster around DONSON (downstream neighbor of SON) contained genes such as SON, CEP164 and CEP192, C20ORF4, TMEM82 and RPA1 (Figure 4a). The two centrosomal proteins CEP164 and CEP192 were recently shown to be required for centrosome biogenesis, spindle assembly and DNA repair (Gomez-Ferreria et al., 2008; Sivasubramaniam et al., 2008). Replication protein A (RPA1) is a known regulator of DNA damage repair and required for replication and cell cycle

progression (reviewed in Binz et al., 2004). Uncharacterized or poorly understood genes within this cluster include DONSON, SON and C20ORF4. Together, they all exhibited similar phenotypes i.e. low cell number, high nuclear intensity and mitotic cells, probably because of cells arresting in a specific cell cycle phase (Figure 4a, compare images in Figure 4b).

a

hgnc	homolog.fly	homolog.worm	n	Cit	Csz	ecc	a2i	Nsz	Nit	NCr	AF	BC	C	LA	M	P
CEP164																
CEP192																
GABRA3	Lcch3															
C20orf4	CG12320	F10B5.2														
DONSON	hd	C24H12.5														
SON																
GORASP2	Grasp65	Y42H9AR.1														
C10orf78																
LOC400492																
APBB1IP																
PSMD1	Rpn2	rpn-2														
OR2G2																
ARHGAP20																
VEPH1	melt	K10B4.3														
MSI2		msi-1														
PSMD6	Rpn7	rpn-7														
APBA1	X11Lbeta	lin-10														
CFL1																
GNA12	cta	gpa-12														
FBXO44		C14B1.3														
CENPI																
TMEM82	rev7															
PSMD3	Dox-A2	rpn-3														
CKAP5	msps	zyg-9														
CCBE1																
NR2C2		nhr-69														
ERAF																
RPA1	RpA-70	rpa-1														
NDOR1	CG13667	fre-1														
ERAF																

b

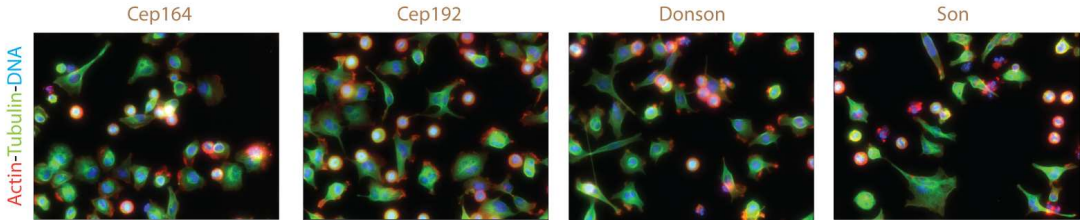

Figure 4 DONSON gene centered cluster. (a) 30 phenotypically closest genes to DONSON perturbation phenotype. If available, putative homologs in *Drosphila* and *C. elegans* are indicated. Phenotypic profiles are shown on the right, with red showing an increase and blue showing a decrease of a feature or class within the well. (b) Representative example images of some genes within this cluster. Note the significantly higher number of arrested cells.

A second gene centered cluster around CASP8AP2 was chosen for follow-up experiments (Figure S1). Examples of genes included in this cluster are ERCC1/ASE-1, RRM1, Prim2A, TMEM61 and SETD8. Several partially characterized genes within this cluster, such as Prim2A, ERCC1 and SETD8, are thought to either be required for S-phase progression and replication or DNA damage signaling (Jorgensen et al., 2007; Gossage and Madhusudan, 2007). Cells in this cluster showed a protrusion/elongation phenotype with an increased cell size (Figure S1).

For the functional characterization of our candidate genes, we performed high-throughput *in-situ* cytometry to identify potential roles of selected genes in specific cell cycle phases, e.g. replication and mitosis. Furthermore, I retested all fly homologs of genes from the DONSON cluster to check for functional conservation. Requirement of conserved genes for cell cycle progression and cell viability in various organisms could help to infer protein function and point towards unknown genes which are required for cell cycle progression under normal and DNA-damage inducing conditions.

2.2 Cell-cycle analysis

2.2.1 DNA content analysis of human cells

To analyze the effect of protein depletion on cell cycle progression, we performed DNA content analysis of RNAi-treated U2OS human cultured cells. For this, a set of about 300 genes with obvious phenotypes from the primary screen were chosen, including the previously mentioned clusters around DONSON and CASP8AP2. Cells were reverse transfected with siRNAs and incubated for 48 hours before analysis to allow for protein depletion. Additionally, siRNA treated replicate plates were irradiated with 10 Gy IR and fixed after 24 hours recovery time (Figure 5a).
For the retest analysis we mainly used siRNA from a different vendor (Qiagen) than the primary screen (Dharmacon) to also assess reproducibility and specificity of and to identify potential off-target effects (OTE) from our primary screen.

An *in-situ* high-throughput cytometer (Acumen Explorer, TTP LabTech) was used for DNA content analysis. Negative (siRLuc) and positive (siPlk1) controls were used for the definition of gates corresponding to cell-cycle phases G1, S and G2/M, as well as cells with sub-G1 and G2+ (aneuploid) DNA content to identify abnormal or apoptotic phenotypes.

Following 48 hours of siRNA treatment, the positive control Plk1, and other known proteins required for entry into and progression of mitosis, such as CDCA8, CDCA5, ANLN and KIF23 showed a very strong G2/M arrest (Figure 5c). Depletion of both subunits of ribonucleotide reductase M1 and M2 (RRM1/2) resulted in a G1/S arrest, similar to the cell-cycle profile of DONSON knockdown (Figure 5b and 5d). CASP8AP2 and TMEM82 RNAi knockdown both showed an increased S-phase reflecting slow progression through S-phase. While CASP8AP2 additionally exhibited an increased G2/M-phase, cells of TMEM82 knockdown were mostly stuck between G1 and S-phases (Figure 5b and 5c).

IR radiation of cells results in DNA double-strand breaks and ATM-mediated activation of DNA repair signaling and checkpoint arrest in G2/M phase (Jaenicke et al., 2001). Cells which were incubated for additional time after IR can re-enter cell cycle after completion of DNA damage repair (DDR) and inactivation of checkpoint pathways. Such cells are synchronized after G2/M arrest. Knockdown of genes required for checkpoint signaling, replication or DDR prior to IR therefore reveals genes implicated in these processes. After 24 hours of recovery time following IR irradiation, cells appeared synchronized and mainly in G2-phase with almost no cells in S-phase and only low to moderate number of cells in G1-phase (Figure 5c). Again, RRM1 and RRM2 showed increased levels of cells in S-phase. Cell-cycle profiles of both genes were differing from each other significantly as opposed to only RNAi gene knockdown. Precisely, RRM1 showed a G1/S arrest, similar to previous RNAi treatment while RRM2 had most of the cells in S and G2/M-phases. Besides, DONSON; DDX48 and CYR61 displayed an increased number of S-phase cells and high numbers of cells in G1-phase. Finally, EIF3S8, a translation initiation factor, showed an increased S-phase content (Figure 5c). Overall, the most frequently found effect was a viability phenotype without additional cell-cycle specific phenotypes (58 %), followed by G2/M (14 %) and S-phase (12 %) specific arrests without apparent effects on cell viability (Figure 5d).

a

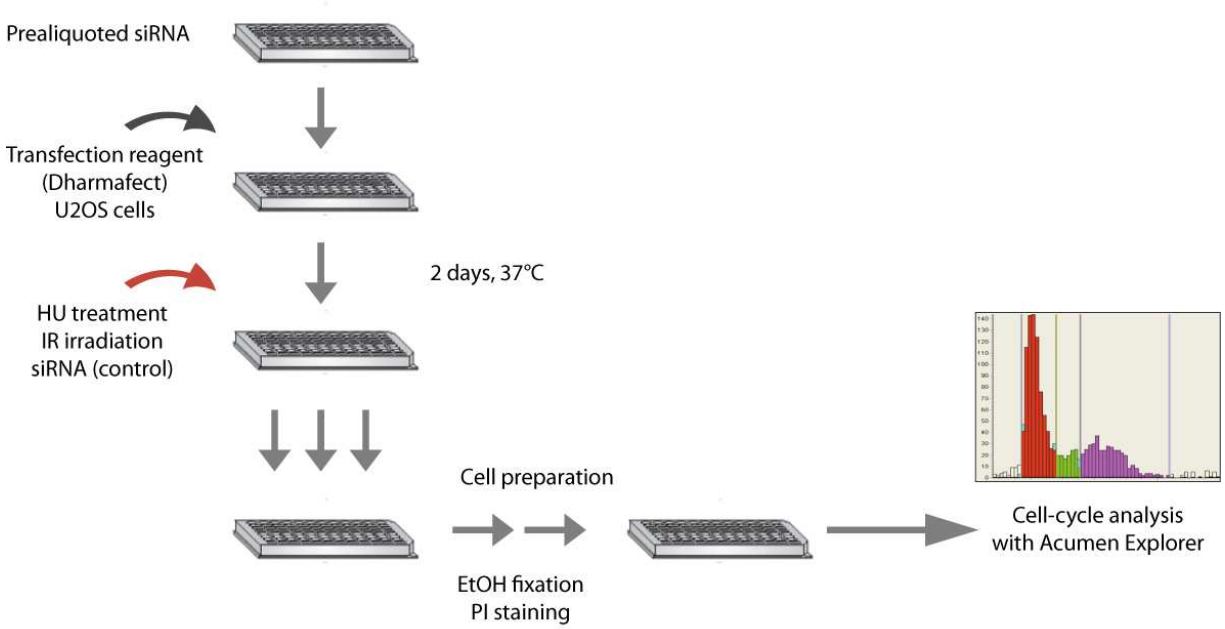
Prealiquoted siRNA
Transfection reagent
(Dharmafect)
U2OS cells
2 days, 37°C
HU treatment
IR irradiation
siRNA (control)
Cell preparation
EtOH fixation
PI staining
Cell-cycle analysis
with Acumen Explorer

b

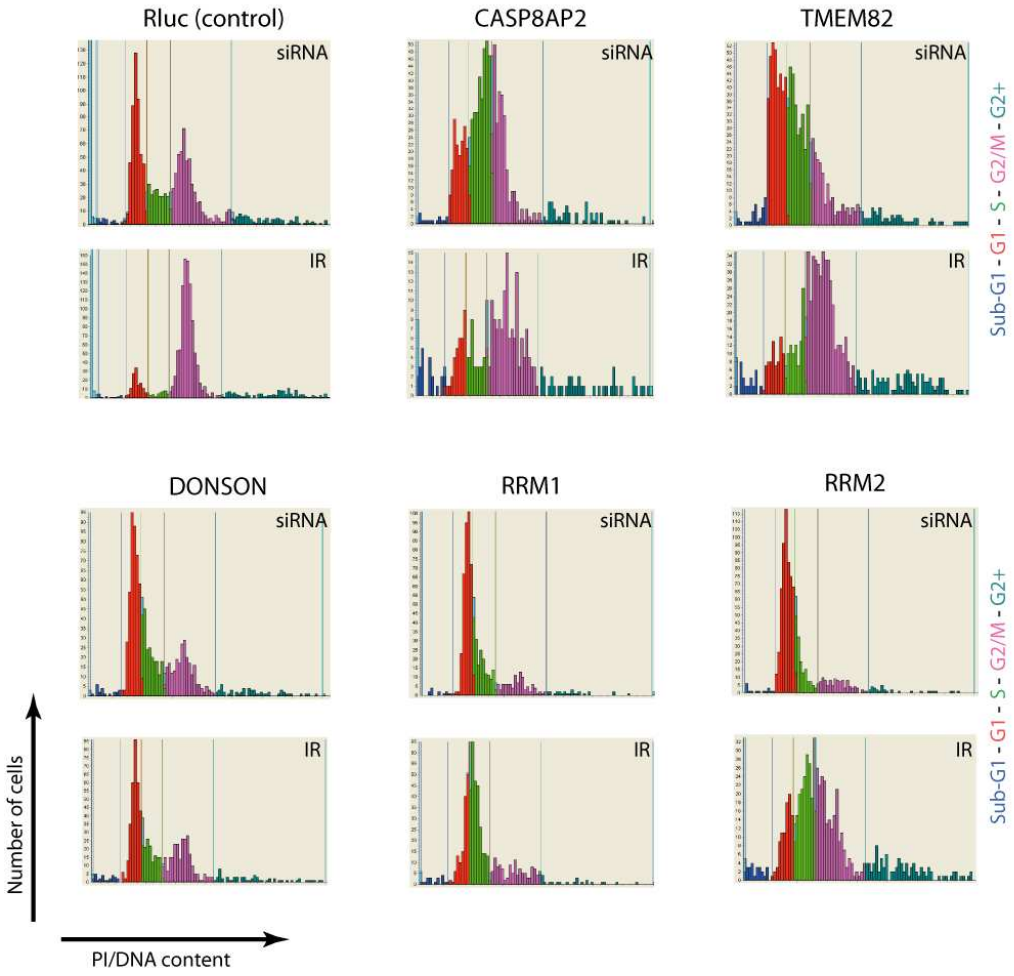
Rluc (control)
CASP8AP2
TMEM82
DONSON
RRM1
RRM2
siRNA
IR
Sub-G1 - G1 - S - G2/M - G2+
Number of cells
PI/DNA content

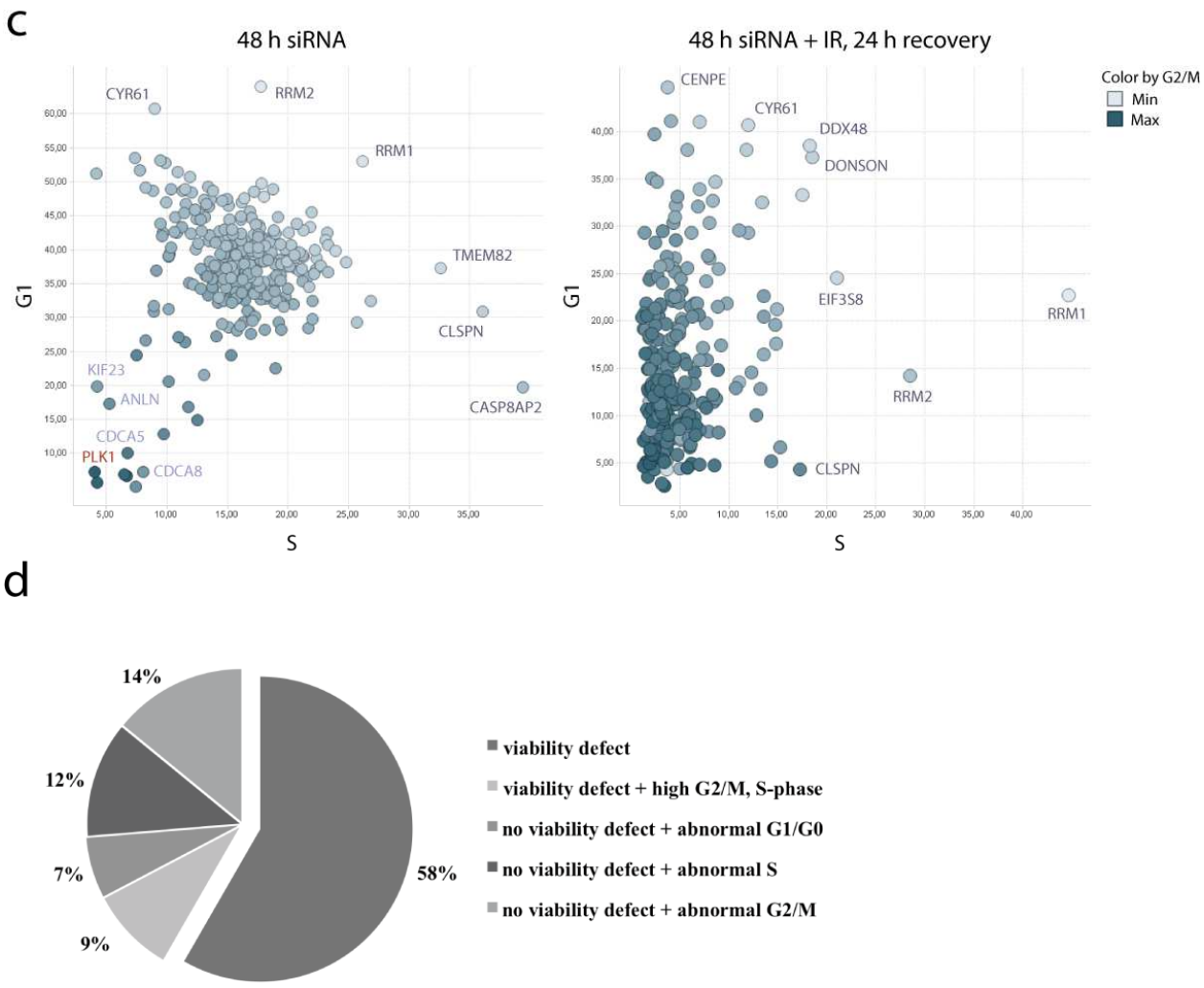

Figure 5 DNA content analysis of candidate genes in human cells. (a) Screening workflow. To identify genes involved in cell cycle and cell viability U2OS cells were reverse transfected with siRNA pools. After 2 days incubation period cells were either treated with Hydroxyurea (not shown), IR irradiated (10 Gy) or incubated for according time periods to the recovery time of IR irradiated plates (24 hours). Subsequently, cells were fixed, stained and subjected to a *in-situ* cytometrical analysis for quantification of the different cell-cycle phases. A high-throughput cytometer (Acumen Explorer, TTP LabTech) was used to analyze 384-well plates. (b) Histograms of genes with cell-cycle effects. CASP8AP2 and TMEM82 showed strong viability phenotypes with increased number of cells with S-phase DNA content. While CASP8AP2 arrests between S and G2/M-phase, TMEM82 appears to be arrested in G1-S transition. RRM1, RRM2 and DONSON knockdown show increased S-phases and decreased G2/M peaks revealing a putative role of those genes in S-phase progression and replication. (c) Scatter plots of all ~300 gene perturbations with and without IR irradiation. Gene names of the strongest outliers are indicated. Samples are plotted against the frequency of cells with G1 and S-phase DNA content. Colors represent proportion of cells with G2/M DNA content. (d) 142 aberrant phenotypes were found and grouped into five different classes, describing the effect of siRNA treatment on cell viability and cell cycle.

Taken together, using high-throughput DNA content analysis we found some of our candidate genes from the primary screen with cell-cycle specific phenotypes including RRM1, RRM2, CASP8AP2, TMEM82 and DONSON. Protein depletion of those genes resulted in strong cell-cycle and viability effects and suggests a general requirement of these genes in cellular processes such as replication and S-phase progression (RRM1/2, Donson), entry into mitosis (CASP8AP2) and cell survival (CASP8AP2, TMEM82).

2.2.2 Flow-cytometric analysis of *Drosophila* cells

To identify genes with conserved function, I performed RNAi experiments in *Drosophila* Schneider S2 cells with homologs of genes included in the DONSON cluster (Figure 4a). Additionally, I chose candidate genes from the primary screen which showed activation of DNA damage signaling upon their depletion (chapter 2.3; for complete list, see Table S1). dsRNAs were generated from a previously published dsRNA library (Boutros et al., 2004; Hild et al., 2003). Following a reverse incubation protocol, S2 cells were seeded in serum-free media to increase dsRNA uptake due to serum-starvation. Cells were incubated for 4 days for knockdown of cellular mRNA levels and protein depletion. One replicate was treated with Hydroxyurea (HU), which induces G1/S-arrest and allows to evaluate synthetic interactions by activating the DNA damage response (Figure 6c). After incubation period, cells were fixed and stained with propidium iodide for flow cytometric DNA quantification (Figure 6a).
Silencing of RpA-70, msps and RnrL, the homologs of RPA1, CKAP5 and RRM1, respectively had a dramatic effect on cell viability (Figure 6b). Cells with sub-G1 DNA content, reflecting apoptotic cells and cellular debris, increased most significantly after depletion of RnrL (28 %) compared to negative control (6 %) (Figure 6e). RpA-70 knockdown induced a strong G2/M arrest concomitantly with cell death (Figure 6b). mini-spindles (msps), the *Drosophila* homolog of CKAP5, showed increased sub-G1 proportion and an elevated G1 peak. The *Drosophila* homologs of three proteasomal proteins PSMD1, PSMD6 and PSMD3, which were found in the DONSON cluster, all exhibited characteristically low levels of S-phase cells and either a weak G2/M arrest (Rpn2 and Rpn7) or a G1 arrest (Dox-A2) (Figure 6d).

a

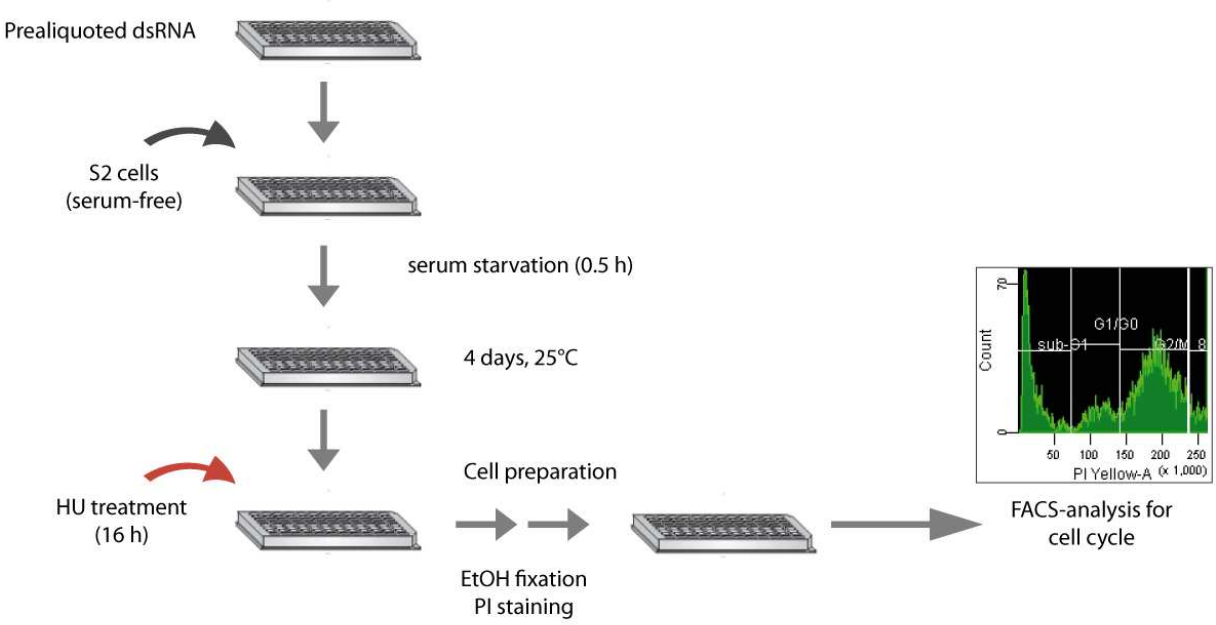
Prealiquoted dsRNA
S2 cells
(serum-free)
serum starvation (0.5 h)
4 days, 25°C
HU treatment
(16 h)
Cell preparation
EtOH fixation
PI staining
FACS-analysis for
cell cycle
Count
G1/G0
sub-G1
PI Yellow-A (x 1,000)

b

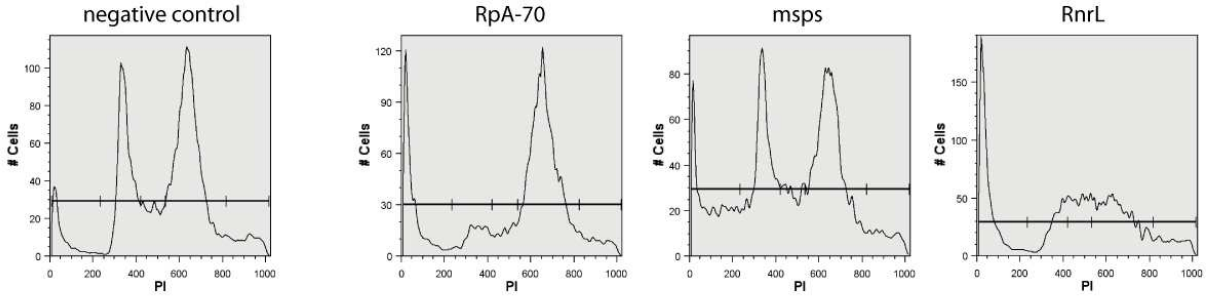
negative control
RpA-70
msps
RnrL
Cells
PI

c

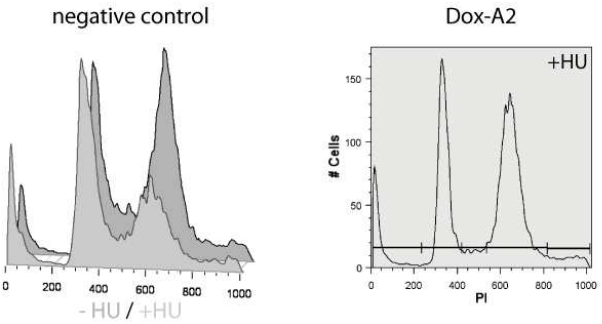
negative control
Dox-A2
+HU
Cells
PI
- HU / +HU

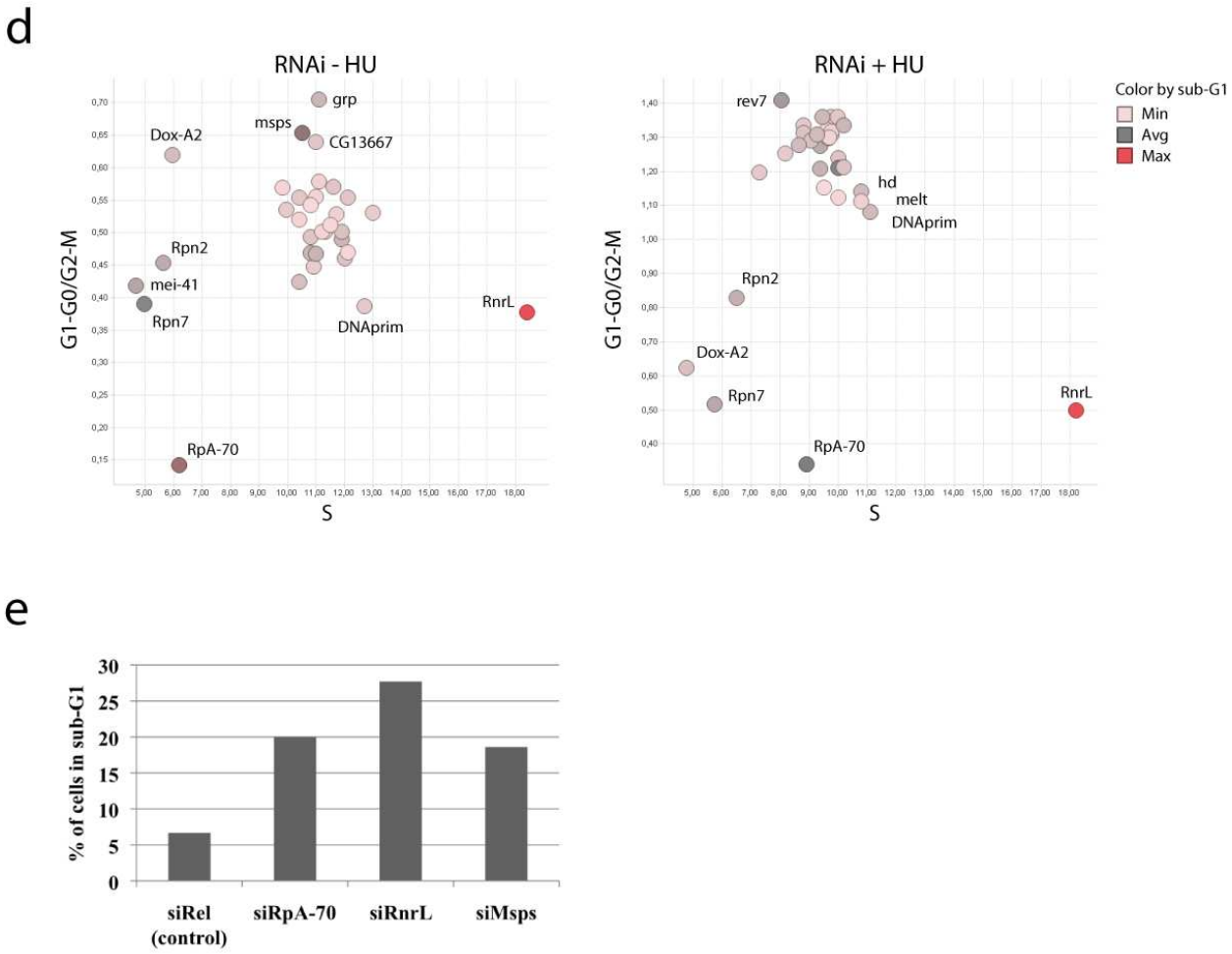

Figure 6 High-throughput flow-cytometric analysis in *Drosophila* culture cells. (a) Experimental workflow. *Drosophila* S2 cells were incubated with dsRNAs in serum-free media to improve dsRNA uptake. After 4 days incubation, 10 mM HU was added and cells were fixed and stained with propidium iodide 16 hours after drug treatment. Cells were subjected to flow cytometrical analysis for quantification of cell cycle phases using a high-throughput capable flow cytometer (BD FACSArray) in 96-well plates. (b) Comparison of histograms obtained from the cell cycle analysis. Knockdown of RpA-70 resulted in a strong G2/M arrest while dsMsps showed an increased G1 phase cell population. Silencing of RnrL produces a dramatic viability effect with a high sub-G1 peak and loss of cells in normal cell cycle. (c) 3D-profile of dsTak1 (negative control) shows a visible G1 arrest upon HU treatment. dsDox-A2 together with HU treatment results in increased number of cells in G2/M-phase compared to RNAi against Dox-A2 without additional drug treatment. (d) Scatter plots of all tested genes with and without HU treatment. Gene names of outliers with obvious cell-cycle effects are indicated. Colors indicate the proportion of cells with sub-G1 DNA-content measured. (e) Cell viability effect of RNAi knockdown. dsRNAs which induced a cell viability or apoptosis phenotype are indicated.

Interestingly, upon additional treatment with HU, while most of the dsRNA samples arrested in G1 phase as expected, all three proteasomal genes showed a marked increase of cells with G2/M DNA content (Figure 6d). humpty dumpty (hd), the *Drosophila* homolog of Donson, did not show any noticeable cell cycle effects, although cell frequency with S and G2/M DNA-content was slightly increased after HU treatment, similar to DNAprim and melted (Figure 6d).

In summary, knockdown of the RRM1 homolog RnrL could partially reproduce the phenotype seen in human cells upon depletion of RRM1. RnrL knockdown showed a much more severe effect on cell viability than the human counterpart. This might be explained by the longer incubation period, higher knockdown efficiency in *Drosophila* cultured cells than in human cells and less genetic redundancy within the *Drosophila* genome. Besides, RNAi against the proteasomal proteins Rpn2, Rpn7 and Dox-A2 resulted in weak cell cycle arrest, visible through low levels of S-phase cells. Synergistic effects upon HU treatment could be observed for dsDox-A2, which switched from a G1 to a G2/M arrested phenotype.

2.3 Fluorescence microscopy reveals genes with effects on genomic integrity

Genomic surveillance mechanisms ensure chromosomal integrity and prevent propagation of aberrant DNA to the daughter cell, which can result from exogenous DNA insults such as DNA damaging agents, UV- and IR irradiation as well as from errors during replication. One central guardian of the chromosome is the DNA repair machinery which can sense DNA damage, activate DNA repair enzymes and transiently arrests the cell, thereby averting entry into S- and M-phases and subsequent integration of mutations into the genome.

Previous findings from our cell-cycle analysis in human and *Drosophila* cells could confirm our hypothesis that loss-of-function phenotypes of genes within our clusters of interest showed cell cycle and viability effects and are required for regular progression through different cell cycle phases. Next, we wanted to test whether activation of checkpoint signaling and DNA damage pathways could account for the observed cell cycle arrest phenotypes of some of our candidate genes.

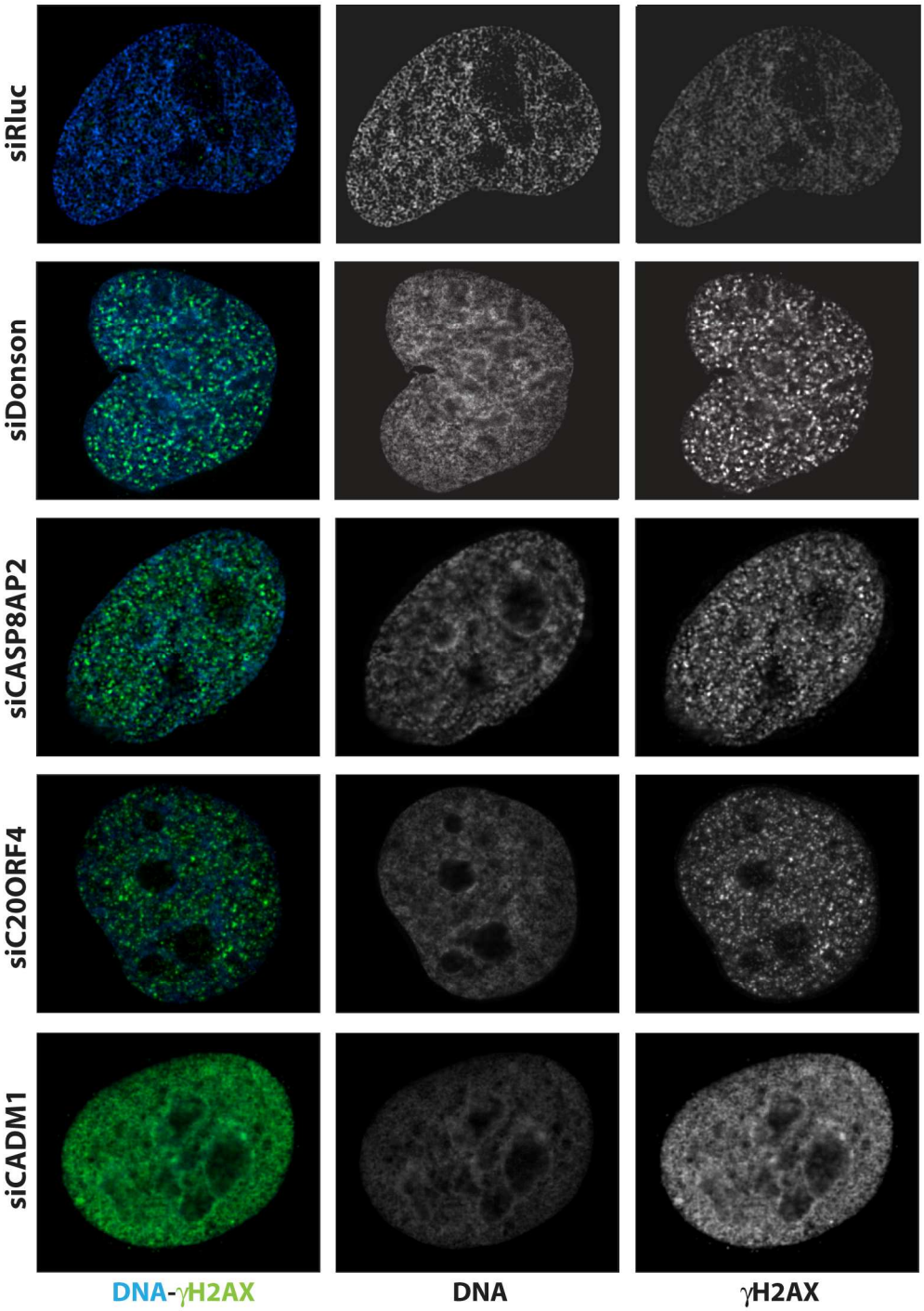

Figure 7 RNAi in U2OS cells reveal genes required for genomic integrity. U2OS cells were incubated for 72 hours following transfection of pooled siRNAs before fixation and staining with γH2AX-specific antibodies and Hoechst nuclear dye. siRluc was used as a negative control. Note that the diffuse staining of siCADM1 treated cells was a general feature of those cells, including replicate cells which were treated with HU.

γH2AX, a DDR-specific H2A-histone variant, is phosphorylated and recruited to DNA damage sites upon DNA insults and serves as a docking platform for downstream signaling components of the ATR and ATM-mediated DDR pathways (reviewed in Fernandez-Capetillo et al., 2004). Phosphorylation of H2AX at its C-terminal tail can be used as readout for DNA damage (Unal et al., 2004). Using phospho-specific antibody against γH2AX and fluorescence microscopy, I checked for DNA damage in human cells after RNAi treatment. For this I used siRNA targeting known DNA damage signaling components such as ATR, ATR, Chek1 and CLSPN and took some of the most interesting genes from our aforementioned phenotypic clusters (DONSON and CASP8AP2 gene centered cluster) including Donson, CASP8AP2, C20ORF4, SON, RRM1, CADM1 and Cep164 (Table 1).

U2OS cells were transfected with siRNAs and incubated for 72 hours before fixation and staining with phospho-H2AX specific antibody and Hoechst as nuclear counterstain. Alternatively, cells were treated with Hydroxyurea 48 hours after siRNA transfection for 24 hours and then either fixed or allowed to recover for additional 8 hours by changing the media prior to fixation.

DNA damage components + controls	Donson cluster	CASP8AP2 cluster
ATM	Donson*	CASP8AP2*
ATR	Top3a	CD3EAP
Chek1	SON	CADM1*
Chek2	Cep164	RRM1
CLSPN	CDCA8*	TMEM61
Rad17*	C20ORF4*	WISP1
WDR33	Prim2A	
DLL4		
Rluc (control)		

Table 1 Genelist for microscopy analysis. Known DNA damage pathway components were included in the analysis. Candidate genes were taken from two gene centered phenotypic clusters around Donson and CASP8AP2. Asterisks indicate cells positive for γH2AX staining after protein depletion.

Most of the tested siRNAs including negative control against Rluc did not show γH2AX staining 72 hours post-transfection (Figure 7). Strikingly, some of the genes we analyzed including Donson, CASP8AP2, C20ORF4 and CADM1 showed a strong formation of nuclear DNA damage foci indicated by dot-like structures located within the nucleus (Figure 7). CASP8AP2 exhibited the strongest response in terms of quantity of visible foci. CADM1, a putative tumor-suppressor gene, revealed a persistent γH2AX staining even after recovery of cells following additional HU treatment (data not shown). HU treatment did not have apparent additive effects with any of the RNAi treatments (not shown). Together these results show that depletion of previously uncharacterized genes such as Donson and C20ORF4 induces strong constitutive DNA damage response. This suggest a role of the above mentioned genes (Figure 7) in preserving genomic integrity and silencing or mutation in those genes might lead to DNA damage and chromosomal instability.

2.4 Functional characterization of Donson

The gene downstream neighbor of SON (DONSON) was found in our genome-wide RNAi screen in a phenotypic cluster exhibiting strong viability effects and cell cycle arrest (Figure 4a). Further analysis of this gene revealed that it is important for progression through S-phase and that depletion of its gene product leads to slow cycling through S-phase and retardation of replication (Figure 5b). Finally, knockdown of Donson induced a strong DNA damage response, visible through the formation of DNA damage foci (Figure 7). Because of the striking perturbation phenotypes of this gene I had a closer look at the gene structure and subcellular localization of its gene product.

The *DONSON* gene locus spans 10 kb on chromosome 21 and lies downstream of the *SON* gene, another yet to be characterized gene. It encodes one transcript for a 566 aa protein. Database searches of the predicted full-length protein revealed that the protein belongs to a conserved family of proteins present in metazoans such as *Drosophila*, *Xenopus* and man (Figure 9a). The human Donson shares 77 % with the mouse protein, 71 % with the Xenopus homolog and 34 % with the *Drosophila* Donson (which is called humpy dumpty, hd) overall sequence identity.

Protein sequence analysis of Donson using the PROSITE database (Falquet et al., 2002) to search for protein domains and functional sites revealed an N-terminal bipartite nuclear localization sequence (NLS), N-myristoylation site at the N-terminus, Ankyrin repeats and multiple putative CK2-phosphorylation sites (Figure 9b).

In order to find out which cellular processes DONSON is involved in, I generated an HA-tagged full-length version of human Donson and cloned it in an expression vector. With this I could not only study localization of Donson within the cell but also perform co-immunoprecipitation experiments to identify putative interaction partners of Donson. Shortly, HA-tagged Donson was generated from a full-length clone (OriGene) using an HA-tagged gene-specific reverse primer. Subsequent digestion of the amplicon and the target expression vector pCDNA3.1(+) (Figure 8a, Invitrogen) using *NheI* and *EcoRI* restriction enzymes and ligation of the insert yielded the appropriate vector product. Successful integration of the insert was checked with colony PCR using gene specific primers (Figure 8b).

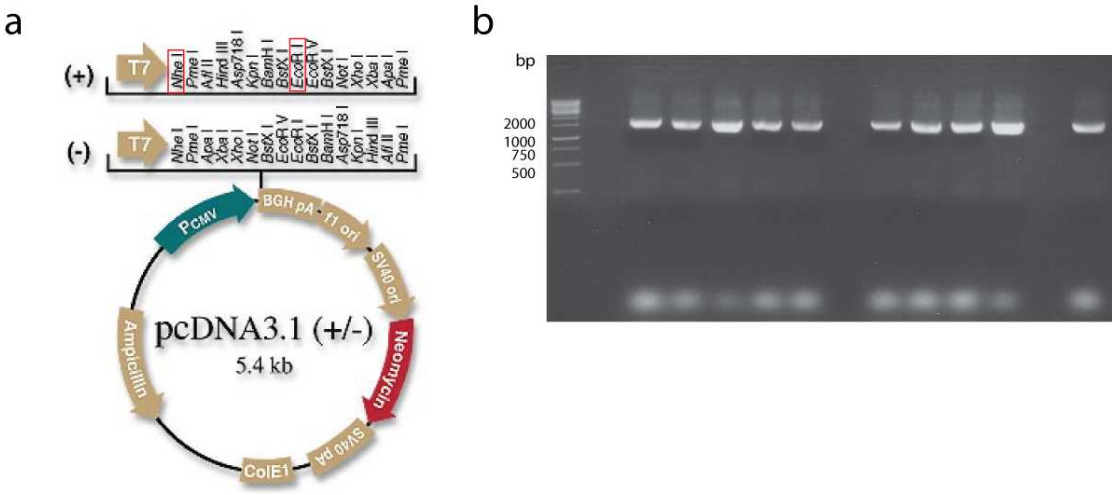

Figure 8 Cloning of human HA-tagged DONSON. (a) Vector map of pcDNA3.1(+/-). The Vector uses a CMV promoter to drive expression. Resistance cassettes for mammalian (Neo^r) and bacterial (Amp^r) systems are available. NheI and EcoRI restriction sites within the multiple cloning region (MCS) was used for digestion and insertion of the cDNA. (b) Results of the colony PCR using gene specific primer pairs. Multiple bacterial colonies were picked and grown for PCR analysis. All tested clones were positive for the insert (~1700 bp).

a

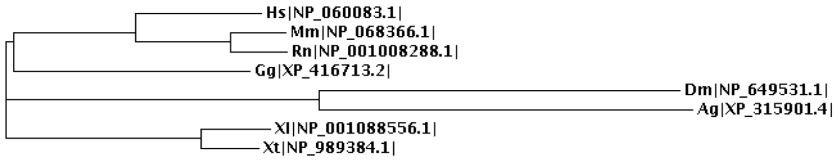

b

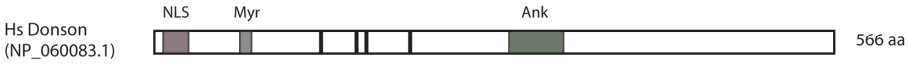

c

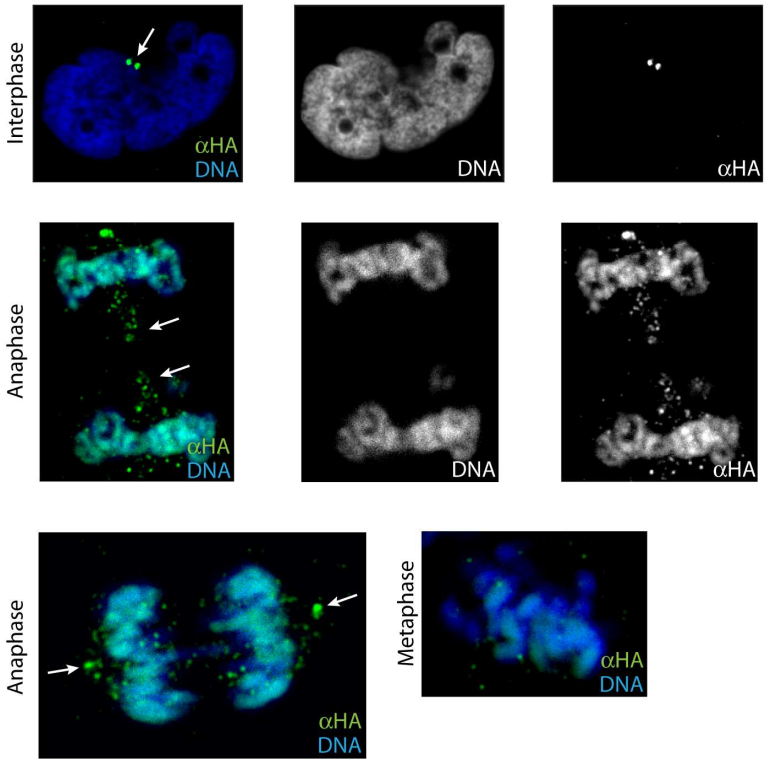

Figure 9 Conservation of DONSON and localization studies. (a) phylogenetic tree of sequences from different species homologs of human DONSON. GeneBank accession numbers are indicated. (b) Predicted structure of human DONSON gene. Black lines represent putative CK2 phosphorylation sites. (c) Localization analysis of HA-tagged DONSON. Arrows indicate the main localization regions of DONSON. Note the diffuse staining in the anaphase cell in the upper panel.

HeLa cells growing on coverslips were transfected with pCDNA-Donson-HA and incubated for 48 hours to allow for gene expression. Cells were fixed, HA-tagged Donson was detected using HA-specific antibody.and DNA was stained with Hoechst dye. αHA-antibody detected a strong signal at the perinuclear region in most of the observed cells. Specifically, two dot-like structures could be seen close to each other and in proximity to the nucleus, reminiscent to the localization of centrioles. (Figure 9c). Mitotic cells showed a broader staining pattern. Beginning in prophase of mitosis, HA-antibody could detect its substrate throughout the nucleus and was colocalizing with chromatin (not shown). In the following stages of mitosis, αHA-antibody staining was almost completely overlapping with DNA (see ‘metaphase’ and ‘anaphase’ images, Figure 9c). In anaphase, two dot-like structures were visible at localization of spindle poles, the prospective destination sides of the segregated chromosomes (Figure 9c, arrows in lower panel). Additionally, diffuse staining could also be detected parallel to the segregation axis and the two spindle poles (Figure 9c, upper panel, arrows). Taken together, localization of Donson as revealed by fluorescence microscopy suggests a centrosomal localization which changes during mitosis to overlap with DNA localization during early and late stages. Consistent with this model, dot-like structures were observed at both spindle poles during anaphase.

3. Discussion

Morphogenesis of tissues and organs in multicellular organisms is based on a complex interplay of different cell populations which communicate with each other and the environment, react to extrinsic cues and adapt to changing conditions. Much like cellular networks, a complicated picture of signal transduction pathways is now emerging with pathways not acting in parallel, independent from each other but working in functional modules with proteins often exerting a multitude of different functions depending on the molecular context (Hartwell, 1999). Reverse genetics has made it possible to systematically screen for novel genes involved in a signaling pathway or cellular process. The most promising reverse genetic perturbation technology, RNAi, allows the identification of genes on a genome-wide scale and supports efforts to understand cellular processes on a systems-level. Besides identifying new genes involved in known signaling pathways, functional genomic studies using RNAi also help in identifying drug targets, often by using so-called synthetic lethal screens, combinatorial screens with chemical compounds or other perturbation reagents (Aza-Blanc et al., 2003). This and other areas of application has made it an attractive approach to systematically attribute functions to genes.

Here, I present a functional analysis of candidate genes based on similarities of perturbation phenotypes of several uncharacterized genes with known genes using image-based quantification approaches and multidimensional profiling of perturbation phenotypes on a single-cell level. Analysis of gene centered clusters around DONSON, an previously unknown gene and CASP8AP2 in secondary assays revealed genes required for cell-cycle progression, genomic integrity and cell survival. Localization studies of DONSON showed that it may localize to centrosomes throughout the cell-cycle, suggesting important roles for DONSON in mitotic entry, checkpoint signaling and centriole duplication. Consistent with its suggested role in cellular survival, silencing of DONSON resulted in strong DNA damage induction and cell-cycle arrest at the G1-S transition point.

3.1 Genome-wide RNAi screen reveals tight phenotypic clusters

Forward genetic studies have contributed much to our current understanding of cellular processes as diverse as cell cycle, secretion, cell motility and signal transduction, to name a few. Core components of the cellular machinery have been identified as well as characterized and put into context of whole organisms in development and disease-related processes. However, a significant portion of the human genome is not functionally characterized and classical mutagenesis screens might be too limiting in their phenotypic readout capacity, and saturation of the whole genome might not be achieved due to preferential 'hits' in specific regions of the genome. Alternative approaches are needed to fill the gap of our current knowledge about biology of cells and organisms. RNAi technology offers a way to systematically and specifically analyze gene function by various phenotypic assays such as colorimetric, chemiluminescent and microscopic readouts (reviewed in Boutros and Ahringer, 2008).

In our current study, we used large-scale RNAi perturbations covering almost the entire human genome to identify novel components of functional modules involved in cell morphogenesis, survival and cell-cycle. Using a supervised learning algorithm, cells were classified in different phenotypic classes. Multi-parametric profiling of gene perturbation phenotypes enabled us to map the phenotypic profile space of the whole screen based on morphological features of single cells. With this approach we could identify several distinct phenotypic clusters which we used as a starting point for secondary assays and functional studies of unknown genes (Figure 4a). Two phenotypic clusters were studied further in detail. One cluster in which genes exhibited a strong viability effect and cell cycle arrest comprised uncharacterized genes such as DONSON, SON and C20ORF4, and the known centrosomal genes Cep164 and Cep192, which were recently found to be important for centrosome biogenesis and duplication as well as spindle assembly and DNA damage signaling (Sivasubramaniam et al., 2008; Gomez-Ferreria et al., 2008). A second gene centered phenotypic cluster contained genes such as CASP8AP2, which is associated with Fas-ligand mediated apoptosis (reviewed in Krieghoff et al., 2007), TMEM61 and RRM1, a subunit of the ribonucleoside-diphosphate reductase, an enzyme essential for the production of deoxyribonucleotides prior to DNA synthesis in S-phase of dividing cells.

Previous functional studies which utilized the RNAi technology to dissect cell morphology and remodeling of cell shapes did either manually score and compare phenotypes (Kiger et al., 2003) or used only a subset of genes for quantitative analysis of cell morphology (Bakal et al., 2007). Our dataset now allows the analysis of genes based on a quantitative description of the perturbation phenotype. This provides an unbiased approach to study gene function and the method used in our study can be adapted to other image-based screens and datasets. One major advantage over reductionistic readouts used to dissect specific cellular pathways using cell-based reporter assays is the general applicability of the image data to analyze a variety of different cellular processes. Additionally, due to pleiotropic effects of single genes, specific gene functions are often missed because of restricted phenotypic readout methods. High-throughput microscopy based screenings will most certainly be more frequently used in the future, partially because of the need for multi-parametric quantitative data not only in functional genomics but also in drug discovery and development (Loo et al., 2007). Technical advances in microscopy technology and image analysis will improve future studies relying on image-based data and will help to establish more advanced microscopic screenings such as time-lapse microscopy to understand underlying mechanisms leading to remodeling of cell shape (Neumann et al., 2006).

3.2 Cell cycle analysis in human and *Drosophila* cells

For the functional analysis of candidate genes derived from phenotypic clusters, we performed high-throughput *in situ* cytometry. DNA content analysis provides an excellent starting point for the identification of genes required for cell cycle progression, replication and mitosis. Previously published studies could show the general applicability and richness of the dataset obtained from this method (Kittler et al., 2007). Therefore, and because genes within the DONSON cluster showed cell cycle arrest phenotypes, we used RNAi and IR irradiation to identify genes which show cell cycle effects upon their depletion. Multiple genes including CDCA5, CDCA8, ANLN and KIF23 showed cell viability phenotypes and G2/M arrest, consistent with their essential roles in mitosis and cytokinesis (Figure 5c). Several candidate genes showed a marked increase in cells with S-phase DNA content after

RNAi treatment. While RRM1, RRM2, TMEM82 and DONSON arrested at the G1/S transition, CASP8AP2 showed a strong increase in cells arrest in S-phase and an increase in cells with G1 DNA content (Figure 5b). RRM1 and RRM2 are both part of an enzymatic complex, ribonucleoside-diphosphate reductase, which is important for the production of deoxyribonucleotides required for replication and DNA repair. It was also shown that RRM2 directly interacts with p53 and accumulates in the nucleus after UV exposure, suggesting a pivotal role for RRM-subunits in DNA repair (Xue et al. 2003). Knockdown of one of those genes is sufficient to arrest cells in G1 phase. TMEM82 and DONSON show a similar cell cycle profile, with TMEM82 having a higher percentage of cells in S-phase, indicating a slow cycling through S-phase. DONSON, which shows an almost identical profile to RRM1 and RRM2 knockdown, therefore might be important for entry into S-phase or might regulate DNA repair e.g. through checkpoint signaling.

Central cell cycle regulatory proteins are often conserved throughout the animal kingdom. Thus, I asked if knockdown of *Drosophila* homologs of genes from the DONSON cluster would show a similar effect on cell cycle and viability of cells. Silencing of the RRM1 homolog RnrL elicited a severe viability effect with almost 30 % of cells having sub-G1 DNA content (Figure 6b and 6e). This effect might be explained by the generally higher knockdown efficiency and longer incubation time in *Drosophila* culture cells than the RNAi experiments in human cells. Nevertheless, the effect of RnrL knockdown in *Drosophila* cells underscores the essential role of this gene in different organisms. RpA-70, the homolog of human RPA1, showed a G2/M arrest and increase in sub-G1 cells (Figure 6b). RPA1 is mainly involved in DNA repair signaling and homologous recombination, but might exert additional functions during DNA replication (Binz et al., 2004). Our results suggest that RpA-70 is also important for cell survival and might play a role during M-phase of the cell cycle. Mini-spindles (msps), the *Drosophila* homolog of CKAP5, is a centrosomal protein which regulates spindle assembly and stability (Zhang and Megraw, 2007). Following RNAi-mediated silencing of msps, G1 peak and sub-G1 cell population increase (Figure 6b). This could hint towards an early role of msps/CKAP5 in cell cycle already during replication, which extends the previous knowledge about this gene as an exclusive mitotic regulatory protein. In conclusion, using high-throughput DNA content analysis, we could identify potential novel regulators of different cell cycle

phases especially S- and M-phases, which suggests a role of those proteins in replication, genomic surveillance mechanisms and mitosis.

3.3 Microscopy analysis of DNA damage induction

The most delicate time-point during cell cycle in which DNA damage can lead to severe effects and consequences for the cell ranging from apoptosis and cell death to mutation in oncogenes or tumor-suppressor genes is during replication. Several redundant control mechanisms ensure genomic integrity and prevent propagation of introduced mutations from exogenous DNA insults or endogenous errors during DNA synthesis (reviewed in Bartek et al., 2004). Additionally, components of the DNA damage pathway including ATR and its downstream kinase Chk1 might be required for normal replication fork progression during unperturbed S-phase (Petermann and Caldecott, 2006). However, recruitment and regulation of checkpoint components to replication forks during unperturbed DNA replication remains obscure.

Based on the results from the primary microscopy screen and the cell cycle analysis of candidate genes, we next asked whether the genes showing an effect on cell cycle progression might be important for genomic integrity. Using phospho-specific antibody against the activated form of H2AX, we looked for induction of DNA damage upon RNAi treatment. Interestingly, several genes induced strong DNA damage foci upon depletion of their gene products (Figure 7). Especially, Donson, CASP8AP2, C20ORF4 and CADM1 showed a strong DNA damage response. Surprisingly, Cell-adhesion molecule 1 (CADM1) was one of the genes which showed a consistent DNA damage response after RNAi and HU treatment following a recovery period (not shown). CADM1 is described as a tumor-suppressor gene which is mutated in multiple types of cancer, e.g. breast cancer and neuroblastomas (Michels et al., 2008). It will be interesting to investigate, which mechanism is responsible for our observed perturbation effect. If CADM1 is involved in DNA damage signaling or regulation of replication, it probably will indirectly regulate core components of these pathways. DNA damage induction after depletion of Donson suggests a role during replication by protecting DNA from insults or replication fork collapses. If this is achieved indirectly remains to be elucidated. A study of the *Drosophila* homolog of DONSON, humpty dumpty (hd), could show similar cell cycle effects and DNA

damage foci formation which we observed, suggesting a conserved function of Donson (Bandura et al., 2005; see below).

3.4 DONSON, a putative centrosomal protein required for genomic stability

The human gene Downstream neighbor of SON (DONSON) is widely conserved in multicellular eukaryotes from plants to human. Analysis of its sequence predicts an NLS-sequence, Ankyrin-repeats, N-myristoylation sites and multiple putative CK2 phosphorylation sites. Since no additional experiments have been conducted to evaluate different sequence motifs within the DONSON gene, it is hard to predict any protein function or regulation of DONSON through these sites. N-myristoylation might be important for subcellular localization (Taniguchi, 1999) and ankyrin repeats might mediate protein-protein interactions. Indeed, INK4 group of proteins, which inhibit and regulate cell cycle progression through binding to G1-specific cyclin-dependant kinases (CDK4/6) harbor ankyrin-repeats (Canepa et al., 2007). Phosphorylation of DONSON by CK2 could regulate its activity and subcellular localization. Consistent with our suggested role of DONSON in regulation of genomic integrity, it was shown that CK2 binds to and phosphorylates BRCA1 and also supports recruitment of MDC1 to DNA damage sites via MRN interaction by phosphorylating it (O'Brien et al., 1999; Chapman and Jackson, 2008). Future studies will have to examine, if one or all of the predicted sequence motifs have functional relevance to DONSON activity in vivo.

One study found DONSON to be upregulated by E2F transcription factors with the highest expression level at the onset of S-phase. Conversely, constitutive expression of either pRB or $p16^{INK4a}$ resulted in a decreased expression of DONSON (Vernell et al., 2003). The same regulatory mechanism was found in the study of the *Drosophila* homolog of DONSON, humpty dumpty (Hd) (Bandura et al., 2005). These studies suggest an important and conserved role of DONSON in regulating genomic integrity mechanisms during replication. This is also consistent with our observed retardation of S-phase entry and DNA damage induction upon RNAi-mediated gene silencing of DONSON. Intriguingly, the study of *Drosophila* Hd could also show that cells lacking the DONSON homolog have proliferation defects and

reduced genomic DNA replication, and cells mutant for Hd exhibit increased numbers of γH2AX foci (Bandura et al., 2005). In contrast to the suggested functional conservation of DONSON, we could not rescue an RNAi-mediated knockdown of single and pooled siRNAs in human cells using a CMV-promoter driven expression vector containing the mouse homolog of DONSON (data not shown; see Figure S2 for determination of knockdown efficiency of single siRNA against DONSON).

To study protein localization of DONSON within the cell, I used an HA-tagged variant of the full-length protein. DONSON-HA localized to the perinuclear region in two discrete foci, reminiscent of centrioles (Figure 9c). Further localization studies in different cell cycle phases revealed an association of DONSON with DNA throughout mitosis and localization of dot-like structures to the spindle poles of the cell. Centrosomal localization of DONSON might be an important hint for follow-up studies. The centrosome is primarily known for its role as a microtubule organizing center but recent evidence draws a much broader picture than previously anticipated. It not only regulates entry into mitosis but also orchestrates cytokinesis, G1/S transition and monitors DNA damage (reviewed in Schatten, 2008). Recently, several studies could confirm a role of the centrosome as a docking platform for multiple kinases and phosphatases with regulatory roles in cell cycle progression and checkpoint activation. For example, Chk1 was found to be recruited to centrosomes after DNA damage induction (Löffler et al., 2007). In contrast, Bandura and colleagues did find Hd protein located in nuclear foci. These conflicting findings may be due to transient localization in nuclear foci upon recruitment to specific sites within the nucleus e.g. replication forks or DNA damage sites. Transient translocation of DONSON through regulation by a yet to be identified protein interaction or phosphorylation by CK2 or other cell cycle and checkpoint kinases could be one explanation of these contradictory results. The suggested model, where DONSON is cycling between the nucleus and centrosomes, fits with the predicted NLS sequence which is required for transport of cargo proteins into the nucleus by importin family members. Future studies will have to investigate which exact role DONSON plays in the regulation of genomic integrity and surveillance mechanisms during replication including DNA damage and checkpoint signaling.

4 Materials and Methods

4.1 Materials

If not stated otherwise, all chemicals were obtained from Sigma. Specific material and instruments are described in the method's section.

4.1.1 Buffers and media

Drosophila complete medium	Schneider's *Drosophila* medium (Invitrogen); 10% fetal calf serium (Gold Category 'EU', PAA), 1% penicillin/streptomycin (Invitrogen)
Fluoromount-G	Southern Biotech
Human complete medium	Dulbecco's MEM (Gibco); 10% fetal bovine serum (Gibco); 50 µg/mL penicillin/streptomycin (Invitrogen); 2 mM L-glutamine
Phosphate buffered saline (PBS)	137 mM NaCl; 2.7 mM KCl; 10 mM Na_2HPO_4; 2 mM KH_2PO_4
RPMI 1640	Invitrogen

4.1.2 Antibodies and dyes

Alexa488-conjugated goat anti-mouse IgG	Molecular Probes (1:500)
Alexa488-conjugated goat anti-rabbit IgG	Molecular Probes (1:500)
Alexa594-conjugated goat anti-mouse IgG	Molecular Probes (1:500)
Hoechst stain	
Mouse anti-phospho-H2AX	Upstate Biotechnology (1:300)
Rabbit anti-HA	Sigma (1:300)
Propidium iodide (PI)	Molecular Probes

4.1.3 PCR primers

PCR primers were synthesized by Invitrogen. Restriction sites are italic. All dsRNA template primer sequences not listed here are available at http://rnai.dkfz.de.

Donson-HA (reverse primer from MWG biotech)
Don-HA forw: 5'-CC*GCTAGC*GCCACCATGGCCCTTTCGGTGC-3'
Don-HA rev: 5'-CC*GAATTC*CTAAGCATAGTCTGGGACATCATAAGGG
TATCCGCCGGATCTCCAATTATAAATGTAGTCTCTC-3'
Donson real-time PCR
Donson forw: 5'-GTCCAGCATTGTAGGGCAAC-3'
Donson rev: 5'-GGCTCTGCTGGAAGGTACAA-3'

4.2 Methods

4.2.1 Molecular biology

If not stated otherwise, all cloning procedures were performed according to standard protocols (Sambrook et al., 1989). Phusion polymerase (Finnzymes) was used for all PCR cloning purposes. For dsRNA template generation, a Taq polymerase (Qiagen) was used. PCR primers were purchased from Invitrogen except the Donson-HA reverse primer, which was ordered from MWG biotech. Sequences are listed in 4.1.3.

Expression construct

pCDNA-Donson-HA was generated by PCR amplification of the full-length human Donson cDNA clone (NM_017613) from the TrueClone Access cDNA library (OriGene) using an HA-tagged reverse PCR primer. The PCR product was subsequently cloned into an expression vector, *pCDNA3.1(+)* (Invitrogen), using *NheI* and *EcoRI* restriction sites.

In vitro transcription

DNA templates were amplified from *Drosophila* genomic DNA using gene specific primer pairs which contained T7 Promoter tags. Templates were transcribed *in vitro* using a T7 RNA polymerase (Invitrogen) for 16 h at 37°C. After *DNaseI* (Fermentas; 0.5U/50 µl reaction) treatment for 30 min at RT, RNAs were purified using RNeasy Mini Kit (Qiagen). Size and quality of the transcripts were checked by agarose gel electrophoresis. Primer sequence information is available at http://rnai.dkfz.de, and in 4.1.3.

Quantitative real-time PCR

For determination of knockdown efficiency of single siRNA targeting Donson transcript, relative expression level was measured using the Universal ProbeLibrary (Roche) and a LightCycler 480 (Roche). For this, $7.5x10^3$ HeLa cells/well were reverse transfected with 20 nM single siRNAs (Dharmacon) against Donson in a 96 well plate and incubated at 37°C for 48 h to allow for protein depletion. Afterwards, cells were resuspended and 6 wells containing the same siRNA were pooled. RNA was isolated using the RNeasy Mini Kit (Qiagen) and 1 µg RNA was taken for cDNA synthesis using Oligo-dT primer and the RevertAid H Minus First Strand cDNA Synthesis Kit (Fermentas, #K1632). Expression level was normalized against GAPDH and HPRT. Primer for real-time PCR was designed using ProbeFinder (Roche). See 4.1.3 for primer sequences.

4.2.2 Cell culture and transfections

U2OS and HeLa cells were maintained in DMEM complete media at 37°C in a humidified atmosphere with 5% CO_2. *Drosophila* S2R+ and S2 cells were maintained at 25°C in *Drosophila* complete media. Human cells were transfected in 24 well plates with 0.5 µg, 1 µg and 2 µg of DNA respectively, using FuGENE 6 (Roche) or in 384 well plates with 50 ng of DNA. siRNA transfection was done in 384 well and 24 well plates with 20 nM siRNA final concentration using Dharmafect (Dharmacon), according to the manufacturer's protocols.

4.2.3 RNAi experiments

RNAi in *Drosophila* cells and FACS analysis

For RNAi experiments in *Drosophila* cells, dsRNAs were generated from DNA templates of a dsRNA library (Hild et al., 2003) by *in vitro* transcription as described (Boutros et al., 2004). Sequence information of all dsRNAs used in the following experiments is available at http://rnai.dkfz.de. The FACS analysis experiment was performed in 96 well flat bottom plates (Falcon, #353075). For reverse transfection, 1 µg/10 µl H_2O of dsRNAs were pipetted. $3.5x10^5$ S2 cells/well in serum-free media was added and serum-starvation was performed for 30 min at RT to enhance dsRNA uptake. Serum-containing media was added after serum-starvation to 100 µl/well final volume and cell were incubated at 25°C for 4 days to allow for protein depletion. For drug treatment, 10 mM Hydroxurea (Sigma) was added to each well and cells were incubated another 16 h. For fixation, cells were resuspended, two replicate wells were pooled, washed with PBS and fixed in 70% Ethanol at -20°C over night. After aspiration of Ethanol, cells were resuspended in staining solution containing 40 µg/ml propidium iodide (Molecular Probes), 0.5 mg/ml *RNaseA* (Sigma) and PBS, and incubated at 37°C for 2 h. plates were stored at 4°C in the dark prior to FACS analysis.

Flow cytometric DNA quantification was performed with a BD FACSArray (BD Biosciences) in 96 well U-bottom plates (Greiner, #650185). 10000 events were measured per well and further analysis was done using FlowJo software. Clotted cells were excluded from further analysis by defining appropriate gates. For gating of individual cell cycle phases, the DNA profile of Tak1, a negative control, was used in each plate.

DNA content analysis in human cells

For DNA content analysis in human cells, cells were fixed with 80% ice-cold ethanol and incubate for 30 min at -20°C. Cells were then rehydrated by washing with PBS two times. After RNaseA digest (100 µg/ml) for 1 h at 37°C, nuclei were stained with PBS containing 10 µg/ml propidium iodide (Molecular Probes) for 15 min at RT. Stained cells were scanned with an Acumen Explorer (TTP LabTech) and manually

gated with the Acumen Software (TTP LabTech) to quantify percentages of cells with G1, S and G2/M DNA content.

Rescue experiments

For rescue studies of Donson depletion phenotype in human cells, U2OS and HeLa cells were transfected with single and pooled siRNA probes against human Donson (20 nM final concentration per well) in 384 well microtiter imaging grade plates (BD Falcon, #353280) using a Multidrop dispensing system (Thermo) as described above and incubated for 24 h at 37°C. Dilution series of a pCMV-SPORT6 vector containing the mouse Donson full-length cDNA clone (imaGenes) was done using FuGENE6 (Roche) and either 5, 10, 20 or 50 µg of the expression vector. Total amounts of DNA were adjusted to 50 ng with an empty vector (pCDNA6, Invitrogen). Cells were incubated for another 48 h before fixation and PI staining for DNA content analysis with the Acumen Explorer as described above.

4.2.4 Fluorescence microscopy

DNA damage analysis

For observation of DNA damage foci formation, $3.5x10^5$ U2OS cells were seeded on coverslips in 24 well plates and transfected with pooled or single siRNAs (Dharmacon, 20 nM) as described above. 48 h post-transfection, cells were subjected to DNA damage inducing agents, 1 Gy ionizing radiation (IR) or 3 mM Hydroxurea (HU). Controls without treatment were prepared in parallel. Cells were either fixed after 1 h (IR) and 24 h (HU), respectively or after additional 6 h recovery time.
Cells were fixed with PBS containing 5% PFA for 20 min, washed with PBS and PBS containing 0.2% Triton-X-100 and blocked with 3% BSA/0.05% TX-100/PBS for 45 min before incubation with anti-γH2AX antibody (Upstate Biotech., 1:300) over night at 4°C. After another washing step with 0.05% TX-100, cells were incubated with Alexa488 goat anti-mouse secondary antibody for 1 h at RT, washed and incubated for 15 min with Hoechst staining solution (Sigma, 1:1000). Coverslips were mounted onto glass slides with Fluoromount-G (Southern Biotech) mounting media. A Zeiss

AxioImager Z1 with an Apotome was used for microscopy analysis. Images were assembled and processed in Adobe Photoshop and ImageJ software.

Localization studies

For localization studies of human HA-tagged Donson, $3.5x10^4$ HeLa cells/well were seeded on coverslips and 0.5, 1 and 2 µg of pCDNA-Donson-HA (see above) was transfected and total DNA amounts were adjusted to 2 µg. 48 h post-transfection, cells were fixed as described above and incubated with anti-HA antibody (Sigma, 1:300) at 4°C over night. After washing with 0.05% TX-100, cells were incubated either with Alexa488 or Alexa594 goat anti-rabbit antibodies for 1 h at RT, before counter-staining the nuclei with Hoechst (1:1000) for 15 min. Mounting of cells and analysis of images was done as indicated above.

References

Abraham, R.T. Checkpoint signaling: focusing on 53BP1. (2002). Nature Cell Biol. 4, E277-E279.

Aza-Blanc, P., Cooper, C.L., Wagner, K., Batalov, S., Deveraux, Q.L., Cooke, M.P. (2003). Identification of modulators of TRAIL-induced apoptosis via RNAi-based phenotypic screening. Mol. Cell 12, 627-37.

Bakal, C., Aach, J., Church, G., Perrimon, N. (2007). Quantitative morphological signatures define local signaling networks regulating cell morphology. Science 316, 1753-56.

Bandura, J.L., Beall, E.L., Bell, M., Silver, H.R., Botchan, M.R., Calvi, B.R. (2005). Humpty dumpty is required for developmental DNA amplification and cell proliferation in Drosophila. Curr Biol. 15, 755-59.

Bartek, J., Lukas, C., Lukas, J. (2004). Checking on DNA damage in S-phase. Nature Rev. Mol. Cell Biol. 5, 792-804.

Bartscherer, K., Pelte, N., Ingelfinger, D., and Boutros, M. (2006). Secretion of Wnt ligands requires Evi, a conserved transmembrane protein. Cell 125, 523-533.

Berns, K., Hijmans, E.M., Mullenders, J., Brummelkamp, T.R., Velds, A., Heimerikx, M., Kerkhoven, R.M., Madiredjo, M., Nijkamp, W., Weigelt, B., Agami, R., Ge, W., Cavet, G., Linsley, P.S., Beijersbergen, R.L., Bernards, R. (2004) A large-scale RNAi screen in human cells identifies new components of the p53 pathway. Nature 428, 431-37.

Bernstein, E., Caudy, A.A., Hammond, S.M., and Hanon, G.J. (2001). Role for a bidentate ribonuclease in the initiation step of RNA interference. Nature 409, 363-366.

Binz, S.K., Sheeham, A.M., World, M.S. (2004). Replication protein A phosphorylation and the cellular response to DNA damage. DNA repair (Amst) 3, 1015-24.

Boutros, M., Ahringer, J. The art and design of genetic screens: RNA interference. (2008) Nature Rev. Genet. 9, 554-566.

Boutros, M., Kiger, A.A., Armknecht, S., Kerr, K., Hild, M., Koch, B., Haas, S.A., Heidelberger Fly Array Consortium, Paro, R., Perrimon, N. (2004) Genome-wide RNAi analysis of growth and viability in Drosophila cells. Science 303, 832-835.

Campisi, J., d'Adda di Fagagna, F. (2007). Cellular senescence: when bad things happen to good cells. Nat. Rev. Mol. Cell Biol. 8, 729-40.

Canepa, E.T., Scassa, M.E., Ceruti J.M., Marazita, M.C., Carcagno, A.L., Sirkin, P.F., Ogara, M.F. (2007). INK4 proteins, a family of mammalian CDK inhibitors with novel biological functions. IUBMB Life 59, 419-26.

Chapman, J.R:, Jackson, S.P. (2008). Phospho-dependent interactions between NBS1 and MDC1 mediate chromatin retention of the MRN complex at sites of DNA damage. EMBO reports, ahead of print.
Cullen, B.R. (2006) Enhancing and confirming the specificity of RNAi experiments. Nat. Meth. 3, 677-81.

D'Amour, D., Jackson, S.P. (2002). The Mre11 complex: at the crossroads of DNA repair and checkpoint signaling. Nat. Rev. Mol. Cell Biol. 3, 317-327.

Downey, M., Durocher, D. (2006). Gamma-H2AX as a checkpoint maintenance signal. Cell cycle 5, 1376-81.

Echeverri, C.J. et al. (2006). Minimizing the risk of reporting false positives in large-scale RNAi screens. Nature Methods 3, 777-79.

Echeverri, C.J., Perrimon, N. (2006) High-throughput RNAi screening in cultured cells: a user's guide. Nature Rev. Genetics 7, 373-384.

Eggert, U.S., Kiger, A.A., Richter, C., Perlman, Z.E., Perrimon, N., Mitchison, T.J., Field, C.M. (2004). Parallel chemical genetic and genome-wide RNAi screens identify cytokinesis inhibitors and targets. PLoS Biol. 2, 2135-43.

Elbashir, S.M., Harborth, J., Lendeckel, W., Yalcin, A., Weber, K., and Tuschl, T. (2001). Duplexes of 21-nucleotide RNAs mediate RNA interference in cultured mammalian cells. Nature 411, 494-8.

Falquet L, Pagni M, Bucher P, Hulo N, Sigrist CJ, Hofmann K & Bairoch A. (2002). The PROSITE database, its status in 2002. Nucleic Acids Res. 30, 235-238

Fernandez-Capetillo, O., Lee, A., Nussenzweig, M., Nussenzweig, A. (2004). H2AX: the histone guardian of the genome. DNA repair (Amst) 3, 959-67.

Fire, A., Xu, S., Montgomery, M.K., Kostas, S.A., Driver, S.E., Mello, C.C. (1998). Potent and specific genetic interference by double-stranded RNA in Caenorhabditis elegans. Nature 391, 806-11.

Fuchs, F., Sklyar, O., Pau, G., Budjan., C., Horn, T., Huber, W., Boutros, M. (2008). Segmenting the genome by quantitative cellular descriptors using large-scale RNAi perturbations. In preparation.

Gomez-Ferreria, M.A., Sharp, D.J. (2008). Cep192 and the generation of the mitotic spindle. Cell cycle 7, 1507-10.

Goshima, G., Wollman, R., Goodwin, S.S., Zhang, N., Scholey, J.M., Vale, R.D., Stuurman, N. (2007). Genes required for mitotic spindle assembly in Drosophila S2 cells. Science 316, 417-21.

Gossage, L., Madhusudan, S. (2007). Current status of excision repair cross complementing-group 1 (ERCC1) in cancer. Cancer Treat Rev. 33, 565-77.

Hammond, S.M., Bernstein, E., Beach, D., and Hanon, G.J. (2000). An RNA-directed

nuclease mediates post-transcriptional gene silencing in Drosophila cells. Nature 404, 293-296.

Hannon, G.J. RNA interference. (2002). Nature 418, 244-51.

Hartwell, L.H., Hopfield, J.J., Leibler, S., Murray, A.W. (1999). From molecular to modular cell biology. Nature 402, C47-C52.

Hartwell, L.H., Mortimer, R.K., Culotti, J., Culotti, M. (1979). Genetic control of the cell division cycle in yeast: V. Genetic analysis of cdc mutants. Genetics 74, 267-86.

Hild, M., Beckmann, B., Haas, S.A., Koch, B., Solovyev, V., Busold, C., Fellenberg, K., Boutros, M., Vingron, M., Sauer, F. (2003). An integrated gene annotation and transcriptional profiling approach towards the full gene content of the Drosophila genome. Genome Biol 5, R3.

Huang, K., Murphy, R.F. (2004). Boosting accuracy of automated classification of fluorescence microscope images for location proteomics. BMC Bioinformatics 5.

Jänicke, R.U., Engels, I.H., Dunkern, T., Kaina, B., Schulze-Osthoff, K., Porter A.G. (2001). Ionizing radiation but not anticancer drugs causes cell cycle arrest and failure to activate the mitochondrial death pathway in MCF-7 breast carcinoma cell. Oncogene 20, 5043-53.

Jorgensen, S. et al. (2007). The histone methyltransferase SET8 is required for S-phase progression. JCB 179, 1337-1345.

Ketting, R.F., Fischer, S.E., Bernstein, E., Sijen, T., Hannon, G.J., and Plasterk, R.H. (2001). Dicer functions in RNA interference and in synthesis of small RNA involved in developmental timing in C.elegans. Genes Dev 15, 2654-2659.

Kennerdell, J.R., and Carthew, R.W. (1998). Use of dsRNA-mediated genetic interference to demonstrate that frizzled and frizzled 2 act in the wingless pathway. Cell 95, 1017-1026.

Kennerdell, J.R., and Carthew, R.W. (2000). Heritable gene silencing in Drosophila using double-stranded RNA. Nature Biotechnology 17, 896-98.

Kiger, A., Baum, B., Jones, S., Jones, M., Coulson, A., Echeverri, C., and Perrimon, N. (2003). A functional genomic analysis of cell morphology using RNA interference. J Biol 2, 27.

Kittler, R. et al. (2007). Genome-scale RNAi profiling of cell division in human tissue culture cells. Nat Cell Biol. 9, 1401-12.

Krieghoff, E., Milovic-Holm, K., Hoffmann, T.G. (2007). FLASH meets nuclear bodies. Cell cycle 6, 771-775.

Kumagai, A., Lee, J., Yoo, H.Y., Dunphy, W.G. (2006). TopBP1 activates the ATR-ATRIP complex. Cell 124, 943-955.

Liu, S., Bekker-Jensen, S., Mailand, N., Lukas, C., Bartek, J., Lukas, J. (2006) Claspin operates downstream of TopBP1 to direct ATR signaling towards Chk1 activation. Mol. Cell. Biol. 26, 6065-64.

Löffler, H., Bochtler, T., Fritz, B., Tews, B., Ho A.D., Lukas, J., Bartek, J., Krämer, A. (2007). DNA damage-induced accumulation of centrosomal Chk1 contribute to its checkpoint function. Cell cycle 6, 2541-48.

Lukas, C., Melander, F., Stucki, M., Falck, J., Bekker-Jensen, S., Goldberg, M., Lerenthal, Y., Jackson, S.P., Bartek, J., Lukas, J. (2004). Mdc1 couples DNA double-strand break recognition by Nbs1 with its H2AX-dependent chromatin retention. EMBO Journal 23, 2674-83.

Michels, E. et al. (2008). CADM1 is a strong neuroblastoma candidate gene that maps within a 3.72 Mb critical region of loss on 11q23. BMC Cancer 8.

Muller, P., Kuttenkeuler, D., Gesellchen, V., Zeidler, M. P., and Boutros, M. (2005). Identification of JAK/STAT signalling components by genome-wide RNA interference. Nature 436, 871-875.

Napoli, C., Lemieux, C., and Jorgensen, R. (1990). Introduction of a Chimeric Chalcone Synthase Gene into Petunia Results in Reversible Co-Suppression of Homologous Genes in trans. Plant Cell 2, 279-289.

Neumann, B., Held, M. Liebel, U., Erfle, H., Rogers, P., Pepperkok, R., Ellenberg, J. (2006). High-throughput RNAi screening by time-lapse imaging of live cells. Nat. Meth. 3, 385-390.

O'Brien, K., Lemke, S.J., Cocke, K.S., Rao, R.N., Beckmann, R.P. (1999). Casein kinase 2 binds to and phosphorylates BRCA1. Biochem Biophys Res Commun 14, 658-64.

Paddison, P.J., Caudy, A.A., Bernstein, E., Hannon, G.J., Conklin, D.S., (2002). Short-hairpin RNAs (shRNAs) induce sequence-specific silencing in mammalian cells. Genes & Dev. 16, 948-58.

Perlman, Z.E., Slack, M.D., Feng, Y., Mitchison, T.J., Wu, L.F., Altschuler, S.J. (2004). Multidimensional drug profiling by automated microscopy. Science 306, 1194-98.

Petermann, E., Caldecott, K.W. (2006). Evidence that the ATR/Chk1 pathway maintains normal replication fork progression during unperturbed S-phase. Cell cycle 5, 2203-09.

Raftopoulou, M., Hall, A. (2003). Cell migration: Rho GTPases lead the way.. Dev. Biol. 265, 23-32.

Sambrook, J., Fritsch, E.F., Maniatis, T. Molecular cloning. (1989). A laboratory manual. Cold Spring Harbor Laboratory Press, New York.

Sancar, A., Lindsey-Boltz, L.A., Ünsal-Kacmaz, K., Linn, S. (2004) Molecular mechanisms of DNA repair and DNA damage checkpoints. Annu. Rev. Biochem. 73, 39-85.

Scales, S.J., Pepperkok, R., Kreis, T.E. (1997). Visualization of ER-to-Golgi transport in living cells reveals a sequental mode of action for COPII and COPI. Cell 90, 1137-48.

Schatten, H. (2008). The mammalian centrosome and its functional significance. Histochem Cell Biol. 129, 667-86.
Sivasubramaniam, S., Sun, X., Pan, Y.R., Wang, S., Lee, E.Y. (2008). Cep164 is a mediator protein required for the maintenance of genomic stability through modulation of MDC1, RPA, and CHK1. Genes Dev. 22, 587-600.

Spirin, V., Mirny, L.A. (2003). Protein complexes and functional modules in molecular networks. PNAS 100, 12123-28.

Starkuviene, V., Pepperkok, R. (2007). The potential of high-content high-throughput microscopy in drug discovery. British J Pharmacol 152, 62-71.

Stucki, M., Clapperton, J.A., Mohammad, D., Yaffe, M.B., Smerdon, S.J., Jackson, S.P. (2005). MDC1 directly binds phosphorylated Histone H2AX to regulate cellular responses to DNA double-strand breaks. Cell 123, 1213-26.

Tanaka, M., Bateman, R., Rauh, D., Vaisberg, E., Ramachandani, S., Zhang, C., Hansen, K.C., Burlingame, A.L., Trautman, J.K., Shokat, K.M., Adams, C.L. (2005). An unbiased cell morphology-based screen for new, biologically active small molecules. PloS Biol. 3, 764-76.

Taniguchi, H. (1999) Protein myrisoylation in protein-lipid and protein-protein interactions. Biophys Chem. 13, 129-37.

Tavernarakis, N., Wang, S.L., Dorovkov, M., Ryazanov, A., Driscoll, M. (2000). Heritable and inducible genetic interference by double-stranded RNA encoded by transgenes. Nature Genetics 24, 180-183.

Timmons, L., Court, D.L., Fire, A. (2001). Ingestion of bacterially expressed dsRNAs can produce specific and potent genetic interference in Caenorhabditis elegans. Gene 263, 103-112.

Timmons, L., Fire, A. (1998). Specific interference by ingested dsRNA. Nature 395, 854.

Unal, E., Arbel-Eden, A., Sattler, U., Shroff, R., Lichten, M., Haber, J.E., Koshland, D. (2004). DNA damage response pathway uses histone modification to assemble a double-strand break-specific cohesin domain. Mol. Cell 16, 991-1002.

van der Krol, A.R., Mur, L.A., Beld, M., Mol, J.N., and Stuitje, A.R. (1990). Flavonoid genes in petunia: addition of a limited number of gene copies may lead to a suppression of gene expression. Plant Cell 2, 291-299.

Vermeulen, K., Van Bockstaele, D.R., Berneman, Z.N. (2003). The cell-cycle: a review of regulation, deregulation and therapeutic targets in cancer. Cell Prolif. 36, 131-49.

Weiss, R.S., Matsuoka, S., Elledge, S.J., Leder, P. (2002). Hus1 acts upstream of Chk1 in a mammalian DNA damage response pathway. Curr. Biol. 12, 73-77.

Williams, B.R: (1997). Role of the double-stranded RNA-activated protein kinase (PKR) in cell regulation. Biochem Soc Trans. 25, 509-13.

Wollman, R., Stuurman, N. (2008). High-throughput microscopy: from raw images to discoveries. J Cell Sci 120, 3715-22.

Yang, D., Buchholz, F., Huang, Z., Goga, A., Chen, C., Brodsky, F.M., Bishop, J.M. (2002). Short RNA duplexes produced by hydrolysis with Escherichia coli RNase III mediate effective RNA interference in mammalian cells. PNAS 99; 9942-47.

Young, D.W. et al. (2007). Integrating high-content screening and ligand-target prediction to identify mechanism of action. Nat. Chem. Biol. 4, 59-68.

Xu, L., Zhou, B., Liu, X., Qiu, W., Jin, Z., Yen, Y. (2003). Wild-type p53 regulates human ribonucleotide reductase by protein-protein interaction with p53R2 as well as hRRM2 subunits. Cancer Res. 63, 980-86.

Zhang, J., Megraw, T.L. (2007). Proper recruitment of gamma-tubulin and D-TACC/Msps to embryonic Drosophila centrosomes requires centrosomin motif 1. Mol Biol Cell 18, 4037-49.

Acknowledgements

I am grateful to my advisor Michael Boutros whose scientific guidance has helped and influenced this work considerably.
This work was carried out in the division of Signaling and Functional Genomics at the German Cancer Research Center in Heidelberg. I thank all my colleagues for the good working atmosphere and helpful discussions. Especially, I want to thank Florian Fuchs who has introduced me to large-scale microscopy screening and the RNAi technology and supported me throughout my stay in the Boutros lab. I am grateful to Sandra Steinbrink for helping me with the FACS experiments, Dierk Ingelfinger and Kubilay Demir for cloning and qPCR experiments. I thank Thomas Horn, Mona Stricker, Kerstin Spirohn and Claudia Blass for assistance with the dsRNA library.
Lastly, I would like to thank my family and friends for support and patience.

Eidesstattliche Erklärung

Ich erkläre hiermit, dass ich die vorliegende Bachelorarbeit selbständig unter Anleitung verfasst und keine anderen als die angegebenen Quellen und Hilfsmittel benutzt habe.

Heidelberg, 07.07.2008

Appendix

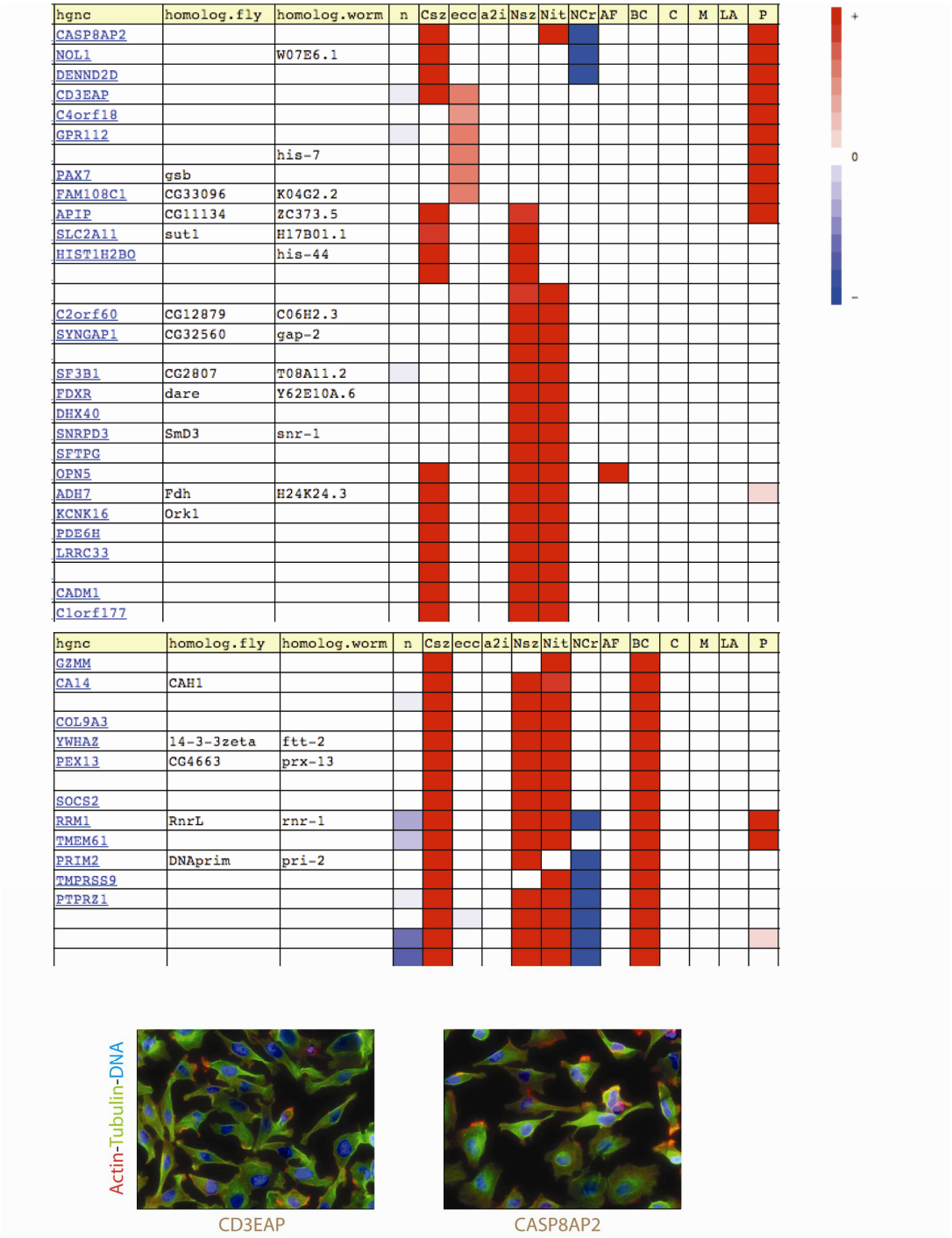

Figure A1 Gene centered cluster around CASP8AP2. (Upper panel) The phenotypically closest genes from CASP8AP2 knockdown phenotype is shown. cells in this cluster have increase nuclear size and a protrusion phenotype. If available, *Drosophila* and *C.elegans* homologs of indicated genes are shown. (lower panel) Example images of two phenotypically close genes, CASP8AP2 and CD3EAP. Phenotypic profiles are on the right, with red showing an increase and blue showing a decrease of a feature or class within the well.

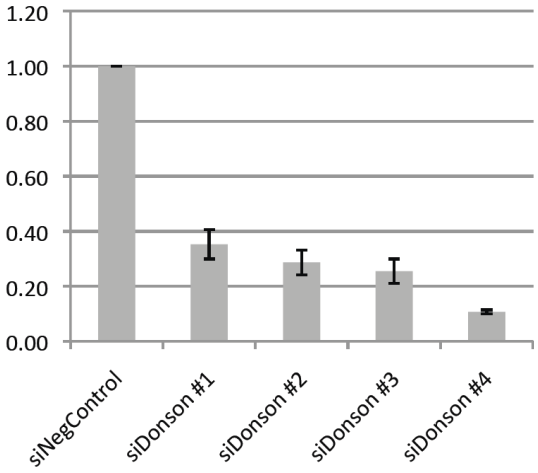

Figure S2 Results from qPCR determining the knockdown efficiency of single siRNAs against DONSON. Four different independent single siRNA (Dharmacon) were tested for the gene-specific knockdown efficiency. Bars show relative amount of DONSON mRNA normalized to GAPDH. siDonson #4 has the strongest effect with 11 % relative mRNA level. Average knockdown efficiency of all 4 siRNA is 25 %.

Gene name (Dm)	Annotation symbol (Dm)	Gene name (Hs)
Lcch3	CG17336	GABRA3
-	CG12320	C20ORF4
hd	CG2669	Donson
Grasp65	CG7809	GORASP2
Rpn2	CG11888	PSMD1
melt	CG8624	VEPH1
Rpn7	CG5378	PSMD6
X11Lbeta	CG32677	APBA1
cta	CG17678	GNA12
rev7	CG2948	TMEM82
Dox-A2	CG10484	PSMD3
msps	CG5000	CKAP5
RpA-70	CG9633	RPA1
-	CG13667	NDOR1
-	CG32251	Clspn
Dll	CG3629	DLL4
lok	CG10895	Chek2
DNAprim	CG5553	Prim2A
Top3alpha	CG10123	Top3a
mei-41	CG4252	ATR
Ercc1	CG10215	ERCC1
RnrL	CG5371	RRMI
grp	CG17161	Chek1
-	CG8273	SON
-	CG1109	WDR33
tefu	CG6535	ATM
Rad17	CG7825	Rad17
-	CG18445	MBOAT2/CADM1
Imd	CG5576	(control)
Rel	CG11992	(control)
Tak1	CG18492	(control)

Table S1 Gene list of fly homologs for DNA content analysis. dsRNAs for negative controls were included in the analysis. Gene name of fly and human homologs are indicated.

List of Figures and Tables